O.Ye. POGORELOV*, O.V. FILATOV, E.M. RUDENKO***,
I.V. KOROTASH****, and M.V. DYAKIN*******

G.V. Kurdyumov Institute for Metal Physics of the N.A.S. of Ukraine,
36 Academician Vernadsky Blvd., UA-03142 Kyiv, Ukraine

*pog.alexander@gmail.com, ** filatov@imp.kiev.ua, *** rudenko@imp.kiev.ua,
  emrudenko@ukr.net, ****korotashiv@ukr.net, ***** max@imp.kiev.ua

CHARACTERIZATION METHODS OF HEAT FLOWS IN SOLIDS

Analysing a wide range of known methods for characterization of the thermal properties of solids, the most effective methods for studying the multilayer systems are determined. Among the considered stationary, quasi-stationary, and non-stationary methods, the Parker's express method for determining the thermophysical characteristics of flat objects and the 3ω method, as well as their modifications for point and planar studies, particularly, of films, are singled out. Parker's modified express method for studying the layered structures makes it possible to reveal the effect of heat-transfer irreversibility within the Cu/AlN/Al system. This effect is explained by the peculiarities of heat-transfer processes at the metal−dielectric interface depending on their Debye temperatures and with taking into account the electron−phonon interaction.

Keywords: thermal conductivity, 3ω method, Parker's express method, temperature measurement, heat-transfer irreversibility effect.

1. Introduction

Efficient transfer of thermal energy is an urgent problem in many diverse problems of energy and solid-state physics. Such problems are specific when multilayer systems and layered and film structures with different thermal and electrical conductivity of the layers are consi-

dered. This is due to the fact that phonon (and in metals and semiconductors also electron) thermal conductivity is affected by thermal resistance at the interface between the layers.

As known [1], the thermal resistance W, which is inversely proportional to the thermal conductivity k of the substance, in layered systems consists of the sum of the thermal resistances of the materials of both the layers W_i and the interfaces between them that the heat flow encounters on its path x. The time of thermal inertia in each of the layers is proportional to the heat capacity c and the density ρ of the substance. Determining the integral value of such time, we can estimate the value of the thermal resistance of the entire system as $W \propto \tau/(c\rho x)$ [1]. On the other hand, the study of heat losses in multilayer structures can be reduced to the study of the features of the passage of heat flows through them, determined by the thermal conductivity coefficient k [1]. The total thermal resistance of a multilayer system can be represented as the thermal resistances of the components connected in series: the thermal resistance of each layer and the thermal resistance of the interface. The thermal resistance to the interface may depend not only on the material of the contacting layers but also on the properties of the interface itself. Taking into account the additivity of the components of the heat supports, it is possible to detect the thermoresistant contribution of the interface. Therefore, first of all, one should consider the existing methods for determining this value and determine the most suitable one for characterizing the thermal resistance of the entire system. Since most of the theoretical foundations of traditional methods have already been considered in Ref. [2], let us dwell on them only by review.

2. Fundamentals of Methods

The study of the process of passage of heat flows through matter is based on the solution of the Fourier equation [1, 3]

$$Q = -k\frac{\partial T}{\partial x}\,; \tag{1}$$

k is the thermal conductivity of the material, T is the temperature transferred along the x-axis. For various physical problems and the geometry of the interaction of a heat flux with matter, the equations are determined by the corresponding limiting and initial conditions, which prompt the choice of one or another research method [3]. There are stationary, quasi-stationary and non-stationary methods, among which analytical and experimental methods can be distinguished.

Analytical methods make it possible to solve a non-stationary problem in any formulation, although they do not differ in high accuracy. Their main disadvantage is that the information about the heat flow ex-

ists outside the experiment and, therefore, cannot be used for current monitoring and control of the thermal process [2].

2.1. Stationary Methods

These methods are divided into those in which heat is supplied to the sample under study from an external heater and those, in which heat is used, which are released in the sample itself, for example, Joule heat, because of the passage of an electric current. The main condition for the application of these methods is to ensure a constant heat flux through-out the entire volume of the sample under study.

In the first case, k is measured in a steady thermal regime, and the sample has the form of a rod (or plate), along the axis of which the heat flux Q is directed. In measurements at low temperatures, small heat losses arising from heat dissipation by the side surfaces are neglected or appropriately corrected for them. At high temperatures, the sample is placed in a heat shield that is maintained at the same temperature. Otherwise, the heating of a thin homogeneous rod, at the ends of which a constant temperature is maintained, occurs by passing an electric current through it. The thermal conductivity coefficient k is determined from the ratio of the temperature difference to the potential difference across the sample. Upon the onset of a stationary thermal regime, the heat balance over the length of the rod dx is described by the equation [2]

$$\frac{d}{dx}\left(k\frac{dT}{dx}\right) + \sigma\left(\frac{dU}{dx}\right)^2 + \frac{\gamma\pi d\Delta T}{\Psi} = 0 \, , \qquad (2)$$

where dU is the potential drop over the length dx, σ is the electrical conductivity coefficient, γ is the heat transfer coefficient of the sample to the environment, Ψ is the rod cross-section. In the absence of heat losses from the surface of the rod, the heat balance equation turns into [2]

$$\left(k\frac{dT}{dx}\right) + \sigma\left(\frac{dU}{dx}\right)^2 = 0 \, , \qquad (3)$$

when k and σ are independent on temperature. With the same temperature of the ends of the rod and the temperature difference between the centre of the rod and its finiteness δT,

$$\frac{k}{\sigma}(\delta T) = 0.5\delta U^2 \, . \qquad (4)$$

The measurement is made in such a way that the current through the sample ensures the stationarity of the temperature distribution in the sample.

2.2. Non-Stationary Methods

They differ from the previous methods in that the non-constant heat flux in the sample determines the change in temperature at each of its points with time. The time during which the temperature changes in a given section of the sample makes it possible to determine its thermal conductivity. The temperature change can be carried out both by continuous and intermittent heat supply. At a constant ambient temperature (T_0 = const), the corresponding solution of the Fourier heat equation [2] is as follows:

$$T_S - T_0 = \sum_{i=1}^{\infty} r_i z_i e^{-m_i t} \, , \tag{5}$$

which for large values of t allows confining to the first member of the series and obtaining

$$\ln(T_S - T_0) = -mt + C \, , \tag{6}$$

where C is a constant, T_S is the sample surface temperature; r_i are constants dependent on the shape of the sample and the initial temperature distribution in it; z_i are coordinate functions characterizing the spatial distribution of temperature in the sample and physical parameters; m_i are constants dependent on the geometry of the sample and characterizing its heat exchange with the environment.

The regular mode of sample temperature change, which occurs when the relative change in temperature at any point of the sample per unit time does not depend on the coordinates of the point and time, provides several methods.

(i) For a heat-insulating ball located in a metal shell, the thermal conductivity coefficient is determined as [2]

$$k = \frac{\gamma R_2}{\left(R_1 \sqrt{\dfrac{m}{a}} \right)\left(1 - \dfrac{m}{\gamma} \dfrac{M_0 c_0}{s_0} \right)} \, , \; a = \phi m; \tag{7}$$

here, ϕ is the form factor; M_0 and c_0 are the mass and heat capacity of the shell, respectively; R_1 and R_2 are the inner and outer radii of the shell, respectively; s_0 is the area of the outer surface of the shell.

(ii) The temperature ratio at two arbitrarily chosen points of the sample does not depend on the time of temperature change, *i.e.* [2],

$$\frac{(T_S - T_0)_1}{(T_S - T_0)_2} = f\left(\frac{m}{a}, x_i, y_i, z_i \right), \tag{8}$$

where x_i, y_i, z_i are the coordinates of two (i = 1, 2) arbitrarily chosen sample points. The use of this method makes it possible to neglect the heat-transfer coefficient.

In the regular mode, the so-called acalorimetric measurement system is used, which involves the use of samples of the correct shape: a cylinder, a prism, a ball, and placing them in a metal shell with high thermal conductivity (copper, silver, brass, *etc.*), providing the temperature control and pre-determining the coefficient forms. This coefficient is determined by the dimensions of the calorimeter or by comparing this calorimeter with the reference one. To do this, a heating acalorimeter is placed in a thermostat and, after certain periods of time, the temperature difference between the cooled sample and the medium is recorded. Based on the data obtained from Eq. (6), a graph $\ln(T_S - T_0) = f(t)$ is plotted, from which the temperature change and the thermal diffusivity are calculated, and from the known ρ and c, the thermal conductivity coefficient k.

2.3. Instant Heat Source Method

To form a heat source for a short period of time t, a heater is turned on, which is built into the sample of the material under study, and its thermal diffusivity a is determined. The heat that has been released in it during this time raises the temperature of the sample, which then decreases because of heat dissipation by it. By measuring the time between turning on the heater and the greatest temperature increase at a point located at a certain distance from the heater, the thermal diffusivity of the sample is calculated by the formula $a = x^2/2t$, where x is the distance of the thermocouple hot junction from the heater. Then, the volumetric heat capacity is determined from the relation [2]

$$\ln(c) = \frac{Q}{2s_h\sqrt{\pi a t_h \Delta T_{\max}}}, \tag{9}$$

where Q is the amount of heat provided by the heater, s_h is the surface of the heater, $\Delta T_{\max}$ is the highest temperature rise at the measurement point, t_h is the time the heater is active.

2.4. Method of Temperature Waves

In this method, the temperature of the heat source changes with a certain period, with which the change in temperature will be repeated at any point of the investigated rod. When certain overall conditions of the sample in the form of a rod are met relative to its cross section and length, the propagation velocity of the first harmonics of the excited temperature waves or the damping decrement of the first harmonics for two temperature waves with different periods in the sample are measured. Such a sample must satisfy the condition of a semi-infinite rod for thermal waves. By simultaneously measuring the mentioned quantities, the coefficient of thermal diffusivity is determined, which has the

form [2]

$$a = \frac{\upsilon d}{2 \ln \lambda_n},$$ (10)

where υ is the velocity of propagation of the temperature wave, d is the distance, at which the temperature is measured, λ_n is the damping decrement of the amplitude of the n-th harmonic of the temperature wave.

2.5. 3ω Method

This thermal-conductivity measurement method is mainly used to measure the thermal conductivity of film structures. The physical and technical principles of the 3ω method are caused by the physical relationship between the voltage drop at the third harmonic of the alternating current (ω is the frequency of alternating current (AC)) on the tape heater and the amount of alternating heat flux (AHF) at the frequency 2ω in the dielectric film, on which this tape heater is applied [4−6]. The alternating heat flow (AHF) in the studied dielectric film, which is determined by its thermal conductivity coefficient k, causes a corresponding change in the temperature of the tape heater, which is caused by heat exchange with the substrate (heat exchange with the environment through air is considered small), and, accordingly, a change in its resistance. Note that the thermal conductivity coefficient of a thin film can significantly differ from the thermal-conductivity coefficient of a bulk material.

The 3ω method assumes the following suggestions [6].

(i) Electric current flows only through the formed metal strip ('hot strip'), which is an electrical resistance heater. In practice, this condition is met, if the resistance of the measured film is much higher than the resistance of the 'hot tape'. Otherwise, the first condition requires electrical isolation of the measured film and the 'hot tape'.

(ii) The transverse dimensions of the deposited metal 'hot tape' are extremely small, namely, of a few tens of microns, that is much less than the thickness of the measured layer (substrate with the film under study).

A harmonic AC $I(t) = I_0 \cos(\omega t)$ is passed through the tape heater (ω is the frequency of AC; I_0 is the amplitude of AC). According to the Joule−Lenz law, during the flow of current during the time dt, heat dQ is released in the tape heater [6]:

$$dQ = I^2(t)R(t)dt.$$ (11)

In this case, the power P released on the tape heater [6] is as follows:

$$P = \frac{dQ}{dt} = I_0^2 R(T)\cos^2(\omega t) = \left(\frac{I_0^2 R(T)}{2}\right)_{DC} + \left(\frac{I_0^2 R(T)\cos(2\omega t)}{2}\right)_{2\omega}.$$ (12)

This power P leads to a change in the temperature of the tape heater and is a superposition of the component corresponding to constant heating and the component corresponding to a temperature change with a frequency doubled relative to the alternating current (the first (DC) and second (2ω) terms in formula (12), respectively). That is, it is possible to record the change in the temperature of the tape heater [6]:

$$\Delta T = \Delta T_{DC} + \Delta T_{2\omega}\cos(2\omega t + \varphi), \tag{13}$$

where ΔT_{DC} is the heater-temperature change due to the direct current component, $\Delta T_{2\omega}$ is the heater-temperature change due to the alternating current component, φ is the phase shift induced by heating the sample mass. The dependence of resistance on temperature in the first approximation has the form

$$R(T) = R_0(1 + \alpha\Delta T), \tag{14}$$

where R_0 is the resistance of the sample at the temperature, at which measurements are made; $\alpha = R^{-1}dR/dT$ is the temperature coefficient of resistance (TCR). From Eqs. (13) and (14), we have

$$R(T) = R_0(1 + \alpha\Delta T_{DC})_{DC} + (R_0\alpha\Delta T_{2\omega}\cos(2\omega t + \varphi))_{2\omega}. \tag{15}$$

According to Ohm's law, the voltage drop U on the tape heater is

$$U = IR = [I_0R_0(1 + \alpha\Delta T_{DC})\cos(\omega t)]_{power} +$$
$$+ \left[\left(\frac{I_0R_0\alpha\Delta T_{2\omega}}{2}\right)\cos(3\omega t + \varphi)\right]_{3\omega} + \left[\left(\frac{I_0R_0\alpha\Delta T_{2\omega}}{2}\right)\cos(\omega t + \varphi)\right]_{\omega}. \tag{16}$$

The resulting Eq. (16) includes a term with a frequency of 3ω, which is proportional to the increase in the temperature of the 'hot strip' [6]:

$$U_{3\omega} = \left[\left(\frac{I_0R_0\alpha\Delta T_{2\omega}}{2}\right)\cos(3\omega t + \varphi)\right]_{3\omega}. \tag{17}$$

Thus, when an AC $I(t) = I_0\cos(\omega t)$ flows through a tape heater with resistance R_0 and TCR α, the temperature change of the 'hot tape' can be determined by measuring the voltage $U_{3\omega}$ at the 3-rd harmonic (3_{ω}) of the AC frequency [6]:

$$\Delta T_{2\omega} = \frac{2U_{3\omega}}{I_0R_0\alpha}. \tag{18}$$

The physical meaning of expressions (17), (18) is that, during the flow of AC through the metal strip-heater, the latter heats up, and due to the positive TCR of the metal, the resistance of the strip-heater increases.

However, since the metal strip-heater and the surface of the test sample have thermal contact, part of the heat passes from the heater to
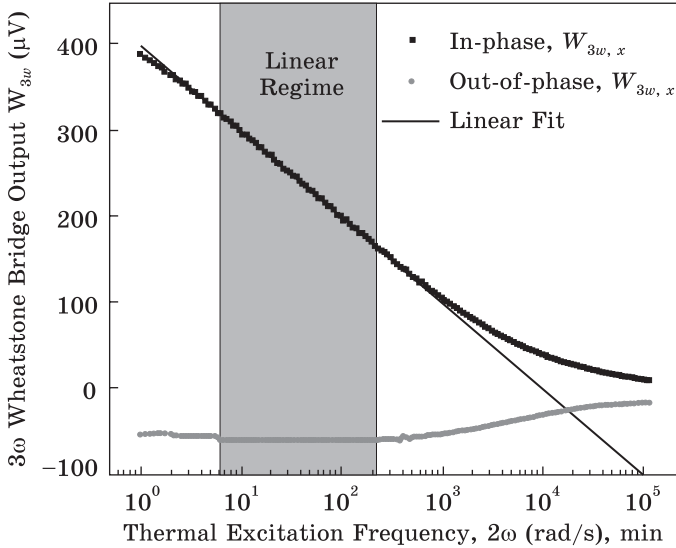
the sample through heat exchange. The amount of heat that the heater gives to the sample, according to Eq. (18), is proportional to the voltage drop at the third harmonic $U_{3\omega}$. In addition, the quantitative characteristic of the heating of the sample is determined by the value of its thermal conductivity coefficient k. By solving the heat-conduction equation for this multilayer system, one can calculate the value of the thermal-conduction coefficient k. This dependence, as shown in Ref. [6], is determined by the dependence of the voltage at the third harmonic $U_{3\omega}$ on the logarithm of the second harmonic $\ln(2\omega)$ (the first term of formula (19)) [6]:

$$U_{3\omega} = -\frac{U_0^3 \, dR/dT}{4R_0^2 l\pi k}\ln(2\omega) + B + i\,\frac{U_0^2}{4lR_0 k}. \tag{19}$$

Other terms in Eq. (19) determine the constant component of the dependence on the logarithm of the second harmonic.

Differentiating both parts of equation (19) concerning the logarithm of the frequency, $\ln(2\omega)$, gives the thermal conductivity coefficient k [6]:

$$k = \left[\frac{U_0^3}{4\pi lR_0}\right]\frac{\alpha\partial\ln(2\omega)}{\partial U_{3\omega}}. \tag{20}$$

Here, l is the length of the sample (heater tape), a is the temperature coefficient of the electrical resistance (TCR) of the heater tape (determined separately), U_0 is the amplitude of the voltage drop across the heater tape with its resistance R_0 and the current $I_0\cos(\omega t)$ that passes through it. The characteristic form of the dependence $U_{3\omega} = f(2\omega)$ is illustrated in Fig. 1 [6].

Let us determine the limits of the permitted frequency ω of the current $I(t) = I_0\cos(\omega t)$ in the experiment. To avoid the effect of heat reflection from the opposite surface of the substrate, it is necessary that the depth of heat penetration into the substrate δ be 5 times less than the thickness d_s of the substrate, *i.e.*, $\delta < d_s/5$. As known, the amplitude of an exponentially decaying function decreases to approximately 1% of its initial value after 5 'length constants'. It can be expected that the magnitude of the thermal fluctuations will decrease below 1% of the initial amplitude after 5 thermal-penetration depths, since the Bessel function decreases faster than the exponential. Thus, the sample thickness, which should be considered infinite, must be greater than 5 times the thermal-penetration depth. Since δ depends on the frequency ω, this condition determines the lower limit ω in the experiment for a substrate with a.

Another condition that imposes an upper limit ω is the requirement for the heater to be a linear source. To do this, the penetration depth δ must be much greater than half the width of the heater b, *i.e.*, $\delta > 5b/2$. Thus, the conditions imposed on the depth of heat penetration can be written as [6]

$$\frac{5b}{2} < \delta < \frac{d_s}{5} \,. \tag{21}$$

The complexity of determining the frequency interval lies in the fact that, to determine the characteristic depth of heat penetration δ, it is necessary to know the numerical value of the thermal diffusivity α of the studied sample that is not known in advance. To solve this problem, it is necessary to measure the voltage at the third harmonic $U_{3\omega}$ as a function of frequency 2ω and to plot the resulting dependence $U_{3\omega} = f(2\omega)$ on a semi-logarithmic scale. As shown in expression (19), the real component $U_{3\omega}$ in a given frequency range (21) depends linearly on the frequency, while the imaginary component is a constant (Fig. 1).

2.5.1. Anisotropy of Thermal Conductivity in Films

To measure the transverse thermal conductivity, we use the 3ω method of variable width of the hot line proposed in Ref. [7].

The authors of Ref. [7] extended the 3ω method to determine the thermal conductivity of thin films both in the plane $k_\parallel$ and across the plane $k_\perp$, if the heater width is changed. The proposed approach makes it possible to measure simultaneously $k_\parallel$ and $k_\perp$ on the same sample. According to the authors of Ref. [7], when the width of the metal strip heater $2b$ is much greater than the thickness of the thin film d_f, the thermal conductivity becomes almost one-dimensional in the direction perpendicular to the film, and $k_\perp$ has a dominant effect on the temperature increase on the sample. On the other hand, in the case of a narrow
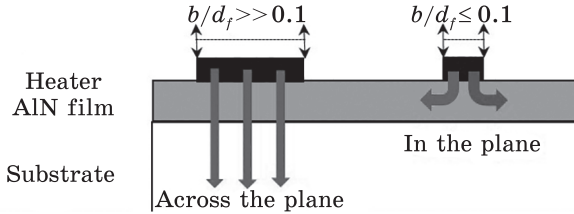
Fig. 2. The scheme of heat flows depends on the half-width of the heater tape [7]

heater, when $b/d_f \leq 0.1$, we can obtain in-plane thermal conductivity data ($k_{\parallel}$). The scheme of heat flows depending on the half-width of the heater tape is shown in Fig. 2.

2.6. Quasi-Stationary Methods

Such methods turn out to be more suitable for the practical implementation of thermophysical measurements. Quasi-stationary conditions are achieved using a pulsed heat source, when the time of passage of a thermal pulse through the sample is so short that the co-authors theoretically substantiated and implemented in Ref. [8] using a flash lamp in the laser flash method (LFM).

The essence of the LFM method consists in heating one of the surfaces of a flat sample ($x = 0$) with a short-term thermal pulse from a powerful flash lamp (ohmic heating, laser, *etc.*) and recording the time dependence of the temperature on the opposite surface of the sample ($x = L$). The theory of the method is based on the use of the temperature distribution in a flat heat-insulated sample, the initial temperature of which is conventionally assumed zero. This makes it possible to significantly simplify the processing of the obtained experimental data, automate the measurement system, and improve the accuracy of the basic flash method.

The temperature distribution equation, on which the 'flash' method is based, is the solution of the corresponding problem of thermal conductivity [3] for a thin flat sample, the heat exchange through the side surfaces of which can be neglected during measurements [8]:

$$T(x,t) = L^{-1}\int_0^L T(x,0)dx +$$
$$+ 2L^{-1}\sum_{n=1}^{\infty}\exp\left(\frac{-n^2\pi^2 at}{L^2}\right)\frac{\cos n\pi x}{L}\int_0^L \frac{T(x,0)\cos n\pi x}{L}\,dx, \tag{22}$$

$$T(x,0) = \frac{Q}{\rho C g} \text{ for } 0 < x < g \text{ and } T(x,0) = 0 \text{ for } g < x < L.$$

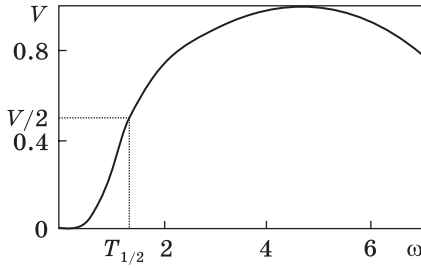On the reverse surface $x = L$, the temperature will change according to the law [8]

Fig. 3. Dependence of dimensionless tempe- rature *V* change on time ω [76]

$$T(L,t) = \frac{Q}{DCL}\left[1 + 2\sum_{n=1}^{\infty}(-1^n)\exp\left(\frac{-n^2\pi^2 at}{L^2}\right)\right]; \tag{23}$$

here, *Q* is the pulse energy density; *t* is the time to reach the set tem- perature value; *a* is coefficient of thermal diffusivity; *C* is the specific heat capacity; ρ is the density of the material; *L* is the sample thickness.

If we go over to dimensionless quantities [8],

$$V(L,t) = \frac{T(L,t)}{T_M} \quad \text{and} \quad \omega = \frac{\pi^2 at}{L^2}, \tag{24}$$

where T_M is the maximum temperature on the reverse surface of the sample, we obtain [8]

$$V = 1 + 2\sum_{n=1}^{\infty}(-1^n)\exp(-n^2\omega). \tag{25}$$

Graphically, this dependence is shown in Fig. 3.

Using this graph and Eq. (25), a formula is obtained for determin- ing the coefficient of thermal diffusivity *a*. The optimal condition, in this case, is the equality $T/T_M = 0.5$. In the case, when the heat losses are insignificant, the relation $t_{1/2} \gg \tau_i$ and the duration of the laser pulse, ω = 1.38, are satisfied. Then, if *V* = 0.5, the value of the thermal diffusivity [8]

$$a = \frac{1.38 L^2}{\pi^2 t_{1/2}}, \tag{26}$$

where $t_{1/2}$ is the time, during which the reverse surface of the sample $x = L$ is heated to half the maximum temperature T_M.

Since the first publication by Parker, many works have appeared, the analysis of which is carried out in Ref. [9], where the method has been subjected to comprehensive research and improvements.

If the above relation is not satisfied, then, the value differs from the one given [10]. For durations $t_{1/2}$ comparable with τ_i, appropriate corrections are introduced [10–13]. As a comparison of Ref. [14] with the data of Ref. [15] showed, the error of the method in practice does not exceed 5%. Some theoretical nuances of the method related to ther-

mophysical studies of samples with coatings are described in detail in Refs. [14, 15].

As follows from (26), to determine only the thermal diffusivity, there is no need to determine the absolute temperature, but only its change on the reverse surface of the sample.

Determining the specific heat capacity at a constant pressure C_P by this method requires additional data, namely, the specific energy Q absorbed by a sample with a specific gravity ρ, when its surface is irradiated with a light flux, determining the maximum temperature T_m and calculating the value using the formula [8]

$$C_P = \frac{Q}{\rho d T_m}.$$ (27)

The thermal conductivity k is determined from the data already established with (26) and (27) from the formula [8]

$$k = a\rho C_p.$$ (28)

To improve the accuracy and reliability of measurements, it is necessary that, if possible, all the energy emitted by the light source be absorbed uniformly and completely by the surface of the sample. For this purpose, blackening of the front surface is used, for example, with colloidal graphite [16], and, in contrast to Ref. [8], the directed radiation of a pulsed laser is chosen as a source.

Usually, as in Ref. [8], the change in temperature is measured with a thermocouple (for example, chromel–alumel) welded to the centre of the back surface of the sample. It is possible to increase the sensitivity of the method by using a battery of thermocouples. In the simplest case, they are welded to the centre of the reverse surface separately at a certain distance (of about 1 mm) that creates a closed electrical circle through the sample. However, there are other methods for increasing the sensitivity of measurements, which involve the use of highly sensitive semiconductor thermocouples and signal amplifiers from thermocouples [17, 18]. In high-temperature measurements, it is advisable to use optical methods using photosensors [20–22] and using an infrared video camera, as described in Refs. [22, 23]. In a case similar to the latter, it is possible to use a precision temperature sensor, namely, a pyrometer of the 'Optris LS' type with a very short thermal-reaction time.

It is possible to increase the reliability of the data obtained by the Parker's method using the processing of the output and amplified signal from the thermocouple using computer technologies using standard packages such as LabVIEW or MathLAB [24, 25].

The effect of various factors (heat losses, radial heat fluxes, sample geometry, *etc.*) on the quality of measurements by the Parker's method

Fig. 4. Temperature change on the reverse surface of the sample depending on τ_i, where the ratio of t to the time the curve reaches saturation is 0.01 (*1*), 0.05 (*2*), and 0.1 (*3*) [26]
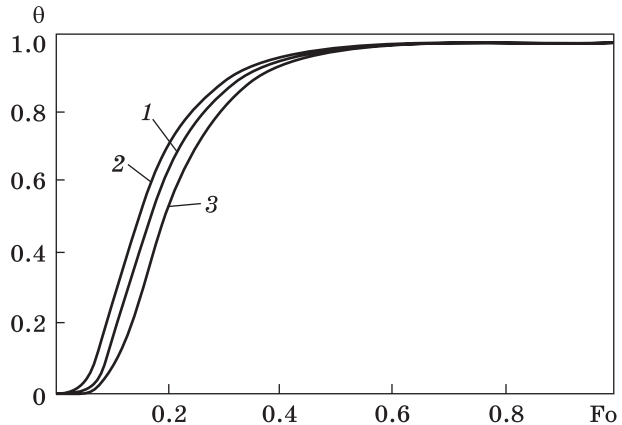
was considered in Ref. [26]. Taking into account that the main parameter, namely, the time $t_{1/2}$, is calculated from the evolution of temperature changes on the reverse surface of the sample, the curve characterizing such changes was analysed. In this work, the analysis of the influence was carried out mainly from the point of view of solving the corresponding problem of heat conduction, taking into account various nuances associated with heat transfer. In the context of the formulated problem, according to the criterion of nonstationarity established in Ref. [27], the laser pulse-duration effect τ_i was the most interesting. The authors of Ref. [26] noted (Fig. 4) that, depending on the magnitude τ_i, the time of the curve reaching the maximum, is different.

Namely, for samples with a high thermal diffusivity, the time it takes for the curve to reach a maximum without heat loss is comparable to the laser pulse duration τ_i. In this case, an increase in τ_i leads to a shift in the heating curve [26].

The conclusions made by the authors of Ref. [26] only based on observations of the shape of the heating curve (Fig. 4) are insufficient and unconvincing from the point of view of the comprehensiveness of the analysis. This is due to the fact that, in this work, the influence of various factors on the thermal diffusivity was considered mainly only based on the results of solving the corresponding problem of thermal conductivity. In this case, the possibility of the influence of structural changes [28, 29], which occur in a substance under the action of a thermal pulse of a certain duration in accordance with the criterion [27] and affect the thermal resistance [30], was not taken into account, and they were not taken into account in the formulation of the corresponding problem of thermal conductivity.

2.6.1. Probing Bulk Samples

For this, the classical Parker's method [8] described above is used. A feature of the method is the probing of a substance by a thermal pulse in a given direction. This makes it possible to study heat transfer depending on the presence of structural defects and their movement under conditions, in which laser-stimulated mass transfer is observed [27].

The dependence of heat transfer on the concentration of foreign atoms was assumed in Ref. [31] and was confirmed experimentally in the 'method for measuring the diffusion coefficient' [32]. The method consisted in determining the thermal diffusivity in the direction of propagation of the probing thermal pulse after sequential removal of layers of a certain thickness Δd and determining D, identifying the change in a as a change in the concentration C of the diffusing substance. The method was developed in addition to methods using radioactive isotopes [33] and was intended for studying the diffusion of atoms, which do not have radioactive isotopes with a long half-life.

The method was tested on measurements of the diffusion coefficient D of carbon and boron in iron, and its verification was carried out by measuring D of radioactive carbon ^{14}C according to the method described in Ref. [33]. Saturation with these elements during stationary diffusion annealing (T = 900 °C) of the surface of iron samples occurred for t = 8 hours. After diffusion annealing, samples with a diameter and a height of 10 mm were turned to a diameter of 5 mm and a thickness of 2 mm in such a way that only one of the flat sides of each sample remained saturated with the diffuser. Diffusion in the direction of penetration of ^{14}C was studied by sequential removal (grinding) of layers of a fixed thickness of 1−1.5 μm parallel to the saturated surface with the measurement of residual radioactivity. The determined diffusion coefficient turned out to be equal to the value $D = 9.22 \cdot 10^{-8} \, cm^2/s$.

To determine the coefficient D of non-radioactive carbon and boron in the direction of diffusion, a chromel−alumel thermocouple was welded to the surface of the samples opposite to the saturated one, the signal from which was fed through a DC amplifier to the input of the recording device. The device was a storage oscilloscope of the S8-13 or S8-14 type synchronized from a thermal pulse source — a solid-state laser with a pulse energy of 2 J and a duration of 1 ms. The laser radiation preliminarily formed by a telescopic system to the size of the cross-section of the sample was directed along the normal to the surface of the sample saturated with the diffusant.

The thermal diffusivity of the samples in the direction of passage of the probing thermal pulse was calculated by Eq. (26) determining $t_{1/2}$ from the recorded oscillogram, and instead of L, the difference

$d_n - \Delta d$ was substituted after each n removed layer. By identifying the change in the value of a_n as dependent on the concentration C of the diffusant, the diffusion coefficient was calculated and, for carbon, was $D = 9.15 \cdot 10^{-8}$ cm^2/s. The error in obtaining the D value by both methods did not exceed a few percent of the tabular value $D = 9.19 \cdot 10^{-8}$ cm^2/s [34, 35]. Therefore, the diffusion coefficient in the direction of penetration of boron into iron was determined similarly and was $D = 3.2 \cdot 10^{-7}$ cm^2/s.

Thus, the determination of D in the direction of penetration of the diffusant, using the flash method, showed the possibility of identifying a change in the thermal diffusivity of a substance depending on the concentration of an impurity in it. The result obtained correlates well with studies [28, 29, 36–38] and the main ideas [30] on the effect of structural defects on the thermal resistance of a substance to a directed heat flow. Such an effect on the heat flux is similar to the effect of defects on mass transfer under conditions of pulsed laser irradiation [39].

2.6.2. Probing of Foils and Films by the Laser-Exited Thermal Pulse

Although the proposed LFM [8] significantly simplified and accelerated the process of obtaining the thermophysical characteristics of monolithic materials, it is impossible to determine the thermophysical characteristics of protective coatings on a product, as well as film elements on substrates. This is primarily due to the fact that expression (26) was obtained in Ref. [8] by solving the heat-conduction equation, which took into account the absorption of laser radiation in the sample material at depths $\delta \ll L$, and the characteristic values of the skin layer δ for metals are of $\sim 10^{-5}$–10^{-4} cm that is comparable and often significantly exceeds the thickness of film elements used in electronics.

For thermal probing of foils, film, thin and nanothickness film samples, the 'Method for express analysis of the thermophysical characteristics of films' was developed for the first time as Patent of Ukraine No. 43224A [40, 41]. The method is as follows (Fig. 5).
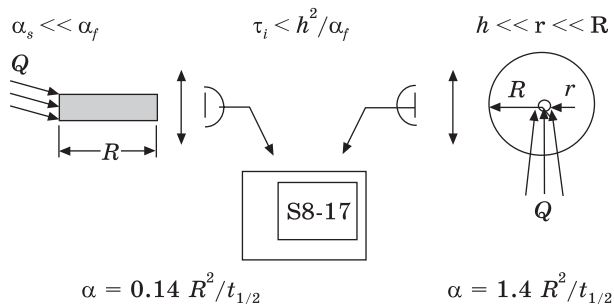

Fig. 5. Improved LFM and its modification for express analysis of thermophysical characteristics of foils and film elements of electronic equipment [40, 41]

$\alpha_s \ll \alpha_f$ $\qquad$ $\tau_i < h^2/\alpha_f$ $\qquad$ $h \ll r \ll R$

S8-17

$\alpha = 0.14\ R^2/t_{1/2}$ $\qquad\qquad$ $\alpha = 1.4\ R^2/t_{1/2}$

As was assumed in [42], the distribution of the radiation intensity over the cross-section of the laser beam is Gaussian, and therefore, the temperature fields arising in the metal under laser action have cylindrical symmetry. This circumstance is essential, when considering the action of laser radiation on films, whose thickness h is commensurate with the thickness of the skin layer δ. Indeed, during the duration of the pulse, heat will be released in a cylindrical region, the axis of which coincides with the axis of the beam. Let us assume that the film has a cylindrical shape, and its radius R is much larger than the thickness, which is assumed to be of the order of the skin layer thickness. Then, if we perform a conformal transformation of this cylindrical region into a rectangular Cartesian one, we come to the LFM scheme, in which $L = \pi R$, and the skin layer thickness is equal to half the skin layer thickness considered in cylindrical geometry.

To use the results obtained in [8], it was proposed to study the rate of temperature rise along the film, taking into account that laser radiation is absorbed instantly throughout the entire thickness of the film. Let us consider the case, when obtaining information about the change in the temperature of the film is carried out at a distance $R \gg h$ — the thickness of the film deposited on the substrate with the thermal diffusivity $a_{\mathrm{s}} \ll a_{\mathrm{f}}$. The solution of the corresponding problem of heat conduction leads to the following relationship [40, 41] for the thermal diffusivity of this film:

$$a_{\mathrm{f}} = \frac{\gamma R^2}{t_{1/2}} \,, \tag{29}$$

where γ is the dimensional coefficient, which is equal to 0.14 for the rectangular film and 1.4 for the disk-shaped film. If the duration of the probing laser pulse $\tau_i < h^2/a_{\mathrm{f}}$ is the stable time of the film, and $R \gg r$ is the diameter of the probing laser beam. Heat abstraction to the substrate during the action of the laser pulse can be neglected, that is, for the study of films with a thickness of several microns, the most effective use of laser pulses of nanosecond duration, and for films with a thickness of more than 100 Å, the picosecond pulses are best.

Knowing the thermal diffusivity of the film and having determined, by analogy with [8], the maximum temperature T_{M} at the controlled point, it is easy to calculate other thermophysical parameters: heat capacity (C) and thermal conductivity (k). The heat capacity C is calculated by Eq. (27), and the thermal conductivity k is calculated by Eq. (28). To determine the specific heat capacity $c_p = C/m$, it is necessary to determine additionally the density of dispersed matter by one of the known methods, for example, using hydrostatic weighing [43].

Approbation of the method was carried out using a modernized layout of the installation, which has proven itself in terms of thermal dif-

Fig. 6. Measuring setup for determining thermophysical characteristics in a vacuum and gaseous medium at different temperatures [41]
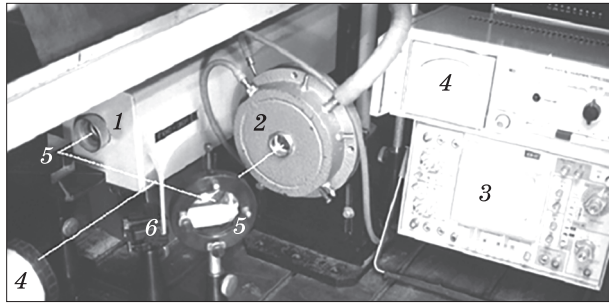
fusivity measurements using the standard LFM for 'thick' samples. The setup (Fig. 6) included a GOS-301 solid-state pulsed neodymium glass laser (**1**) (λ = 1.06 µm) with forming optics, a vacuum chamber (**2**) with a sample holder, an optical system that ensures the formation of a laser beam, targeted irradiation samples and temperature registration scheme. The required duration of the probing laser pulse τ_i = 50 ns was provided by introducing a phototropic shutter into the GOS-301 laser cavity. Temperature changes were recorded using a pyrometric photodetector focused by a lens into a given area of the film and connected *via* a DC amplifier to the input of a C8-17 storage oscilloscope (**3**). To select accurately the focusing region, the optical axis of the pyrometric system was aligned with the optical axis of an aiming low-power laser whose radiation was focused on the chosen region of the film. The energy density of the probing laser pulse Q was determined using an IKT-1N calorimetric meter (**4**). The optical scheme, which consisted of rotary prisms (**5**) and a light-separating plate (**6**), makes it possible to direct the laser beam both for recording its power by a meter (**4**) and for recording by an oscilloscope (**3**) the time $t_{1/2}$ of reaching the temperature $T_{\mathrm{M}}/2$. The operating mock-up of the measuring setup makes it possible to carry out studies both in a gaseous medium and in a vacuum at various temperatures, which was ensured by the location of a nichrome wire heater around the sample [41].

The method can be useful for thermal pulse scanning of film media using new materials and control of other products with coatings, and allows you to study and control films during their deposition. With some modification, the method can be used to characterize tangentially the adhesion of a film or coating to a substrate.

2.6.3. Probing of Foils and Films with the Electric-Spark-Excited Thermal Pulse

Based on the technique described above and the excitation of a thermal pulse, a method was developed for determining the thermophysical characteristics of a metal film or foil [44], in which a probing thermal pulse was generated by an electric spark. The basis for the development of this technique was that, in the previous case (section 2.6.2), it is not

always possible to control the duration of the thermal pulse in the required range to take into account the relaxation capabilities of the film or foil material. In view of the criterion [27], neglecting the thermophysical properties of the material can lead to the formation of numerous structural defects in it and misrepresent the thermophysical characteristics of the integral material of the film or foil.

Therefore, to implement the method in the method for determining the thermophysical characteristics of a metal film or foil, it includes: heating a sample with a thickness L by a thermal pulse with a controlled energy density Q absorbed by the sample surface s, on which the thermal pulse is excited, measuring the temperature change of the sample at a distance from the region s, measuring time $t_{1/2}$, during which this temperature reaches half of its maximum value T_{m}, with a preliminary determination of the average thermal diffusivity a_{f} of the material of the film of thickness L, the pulse energy is directed to the edge of one of the narrow sides of the rectangular film b of length $r \gg b \gg L$ or to the centre of the film of a disk-shaped sample with a radius $r \gg L$, and s is much less than the area of the entire film S, the temperature change is recorded in the direction along the film at the opposite edge from the laser-irradiated area, and the thermal diffusivity and other thermophysical characteristics of the film are determined. But, in contrast to [40, 41], a metal film or foil is heated by an electric discharge with the duration of the discharge pulse (t), which is preliminarily determined from the criterion [27] and the discharge energy (E) according to the relation [27]

$$E \le \frac{kT_{\text{melt}}s}{2\sqrt{a \, / \, t}} \,, \tag{30}$$

where T_{melt} is the melting temperature of the film or foil material, k is the thermal conductivity of the film or foil material, s is the area of the film or foil in the electric discharge region, $t_{1/2}$ is measured and calculated a from (26), and then, calculated and corrected from [27] discharge pulse duration and remeasurements.

2.6.4. Thermal Impulse Sounding of Materials on Substrates for Express Measurements of Their Thermophysical Characteristics

The need to increase the information density of magnetooptical media determines the search for and use of new materials, and the specifics of the recording process, namely, knowledge of the thermophysical characteristics of a film information medium on a compact disc (CD). The correlation of the electrophysical characteristics of the carrier with the thermal characteristics of the medium and disk will ensure the reliability and duration of information storage under conditions of long-term operation of the carrier.

The optimization is based on the analysis of the dynamics of the temperature front propagation in a metal film after irradiation of the film–dielectric substrate system with a laser pulse. The heat-conduction problem for such a system has the form [45]

$$\frac{\partial T_{1,2}}{\partial t} - a_{1,2}\frac{\partial^2 T_{1,2}}{\partial t^2} = \frac{q_{1,2}(z,t)}{\rho_{1,2}C_{1,2}}, \tag{31}$$

where indices 1 and 2 are in accordance with the film and substrate; a is thermal diffusivity, ρ is the density, c is the heat capacity, z is the thickness co-ordinate, r is the co-ordinate along the surface, q is the density of the light flux absorbed in the film and uniformly distributed in its thickness h:

$$q_1 = \frac{q_0 A_1}{h}, \tag{32}$$

and in the lining,

$$q_2 = q_0\left(1 - R_1 - A_1\right)\exp\left[-a_2\left(z - h\right)\right]; \tag{33}$$

R and A are the reflection and absorption coefficients of the material, respectively, and q_0 is the power density of the incident light flux. Under appropriate limiting and initial conditions, the temperature in the film changes according to the general law. If a laser pulse with duration of 10^{-4} s irradiates an opaque film on a substrate, the film is heated to a temperature $T = q_0 A_1 t/(\rho_1 c_1 h)$. Estimates show that, if the film thickness is comparable to the laser pulse absorption depth, its heating with depth occurs almost instantaneously. In this case, it is impossible to measure the thermophysical parameters by the laser flash method (LFM) [8], which uses the analysis of the temperature-front propagation velocity by the z co-ordinate, therefore, to analyse the rate of propagation of the temperature front along the film surface irradiated by a laser.

3. Results and Discussion

3.1. Practical Implementation
of the Characterization of Thermophysical Properties

3.1.1. Laser-Excited Thermal Pulse

The improvement of LFM and its development for the express analysis of the thermophysical characteristics of film elements of electronic equipment was carried out based on works [40, 41].

The measurements were carried out on two types of specially made samples, which were standard polycor substrates of $24\times30\times0.5$ mm in size with metal films deposited on them through a rectangular mask with windows of 3×5 mm (one type of samples) and a round mask with

windows of $\varnothing 5$ mm (another type of samples) 1 µm thick. Metals with well-studied thermophysical characteristics were used as model metals: chromium ERH and iron-Armco, which were sputtered by an electron beam in a VUP-5m vacuum unit at a residual pressure of $(2-5)\cdot 10^{-5}$ Torr on substrates preheated to 150–200 °C.

Using the developed technique described in Section 2.6.2, the first type of specimens makes it possible to simulate the case of heat propagation similar to that considered in [8] for 'thick' specimens. This was motivated by the fact that, if the thermal diffusivity of the substrate $a_2 \ll a_1$ in the film, then, when heat propagates along $r \gg h$ — the film thickness, the heat removal by the substrate during the experiment can be neglected. Rectangular films were irradiated with a laser beam focused by a cylindrical lens into a narrow strip 3 mm long onto the narrow edge of the rectangle. Temperature changes were recorded on the opposite side of the rectangle. Samples of another type were irradiated with a spherical lens, forming a region of $\varnothing 0.1$ mm in the centre of the round film. The change in temperature in the radial direction was recorded at the edge of the film disk.

The high sensitivity of the setup temperature recording circuit (Fig. 6) makes it possible to carry out measurements at $\Delta T < 10$ K with an error not exceeding 8%. This makes it possible to obtain the thermophysical characteristics of materials with phase transitions in a wide temperature range without changing their properties.

The measurements were carried out on two types of specially made samples, which were standard polycor substrates of $24 \times 30 \times 0.5$ mm in size with metal films of 1 µm thick deposited on them through a rectangular mask with windows of 0.3×3 mm and a round mask with windows $2r = 3$ mm. For the fabrication of model films, metals with well-studied thermophysical characteristics were used: Cr and Fe-Armco, as well as Fe(70%)–Cr(30%) and Fe(80%)–Co(20%) alloys, similar in composition to the alloy used in the fabrication of an amorphous Tb–Fe–Co film for magnetooptical recording [46]. Deposition of metal films was performed by an electron beam in a VUP-5m vacuum unit at a residual pressure of $\cong 7 \cdot 10^{-3}$ Pa on substrates preheated to 450 K. The resulting rectangular films were emitted by a laser beam focused by a cylindrical lens into a narrow strip 0.3–0.1 mm in size onto the narrow edge of the rectangular film. Temperature changes were recorded on the opposite side of the rectangle. Samples of another type were irradiated with a spherical lens, forming a region $2r_0 = 0.1$ mm in the centre of the rounded film. The change in temperature in the radial direction was recorded at the edge of the film disk.

The result of studies [47] of the thermal diffusivity of Fe, Cr, Co, and Al films, as the most common metals, which are the base of materials for magnetooptical information carriers, is shown in Fig. 7.

Fig. 7. Temperature dependence of the thermal diffusivity of films [47]: dots of different shapes — experiment; solid curve for Fe — data from Ref. [48]

As can be seen from this figure, the experimental points with a confidence interval obtained for the thermal diffusivity of the Fe film are in good agreement with the data (solid curve) obtained in [48], almost coinciding with the phase-transition point. Thus, the method can be useful for scanning magnetooptical information carriers with a thermal laser probe using new materials as recording media designed to increase the density of recorded information. Due to its high sensitivity, the method can also be used to test other coated products. The developed technique makes it possible to use it for the study and control of films during their deposition.
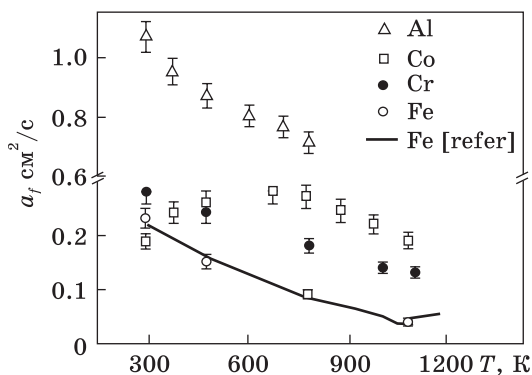
The temperature source formed in the film upon irradiation with a laser pulse can be considered as the initial one for the substrate. Since the substrate is a semi-infinite medium compared to the film, the results of Refs. [49–51] were used to analyse the thermally stimulated processes in it. They obtained a 3-dimensional distribution of the stress field in a semi-infinite condensed absorbing medium, the surface of which was irradiated by a laser pulse. The stress arising in this case in the substrate material is characterized by the corresponding temperature gradients.

Bulk stresses in the substrate and radial stress developing in the film (in the central part of the interaction region, the material is stretched and compressed to its periphery) can lead to its delamination, destruction, and, as a result, to the loss of part of the information. A distinctive feature of the technique is the possibility of using it to monitor the information carrier and the film adhesion to the disk in recording data with a laser beam. In this case, standard CD recorders with appropriate software can be used as monitoring hardware. This is shown schematically in Fig. 8. The analogue-to-digital converter (ADC), to which the photosensor signal is applied, registers the distance r, at which the temperature increase reaches half of its maximum value T_{max}, as well as the time $t_{1/2}$ during which this occurs.

The parameters obtained at each point of the disk are fed to the PC, which calculates the temperature of the film information carrier according to a given algorithm, taking into account the modified boundary
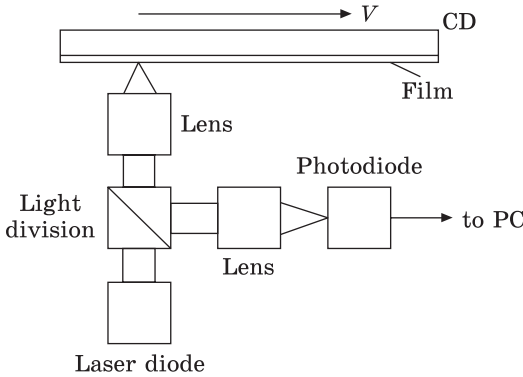
Fig. 8. CD quality control scheme [47]

value problem of thermal conductivity on the radial propagation of heat in an unlimited film irradiated locally with a laser pulse. As the carrier moves at a speed of V, the results of preliminary measurements of the magnitude from point to point are sequentially compared in the PC. By differentiating these data, the quality of adhesion of the film carrier to the disk is controlled. Taking into account the hardware composition of recording laser players, control over the adhesion of the working medium to the base of the discs can be implemented using a special testing program.

The proposed method may be useful for developers of new materials, which are available in too small quantities, but sufficient for the deposition of the film sample under study. It should be noted that, if it is necessary to obtain the thermophysical characteristics of multicomponent materials for film deposition, a method is required that preserves the stoichiometry of their composition, for example, ion-plasma one. The method will be useful for scanning magnetooptical information carriers with a thermal laser probe using new materials as a recording medium, including multilayer ones designed to increase the density of recorded information. The high sensitivity of the temperature recording circuit allows measurements at $\Delta T \leq 10$ K with an error not exceeding 8%. This makes it possible to obtain thermophysical characteristics of materials having phase transitions in a wide temperature range without changing their properties. Due to its high sensitivity, the method can also be used to test other coated products. It is possible to use varieties of the method for non-contact and non-destructive testing of the adhesion of coatings or films to a substrate. The developed technique makes it possible to use it for the study and control of films during their deposition.

3.1.2. Thermal Impulse Excited by an Electric Spark

Probing by a thermal pulse excited by an electric spark, according to the method described in Section 2.6.3, was carried out as follows [44]. Based on the reference data on the melting temperature and thermal diffusivity of the base material of the metal film or foil, the thermophysical characteristics of which are determined, the region 'sample' (Fig. 9) of
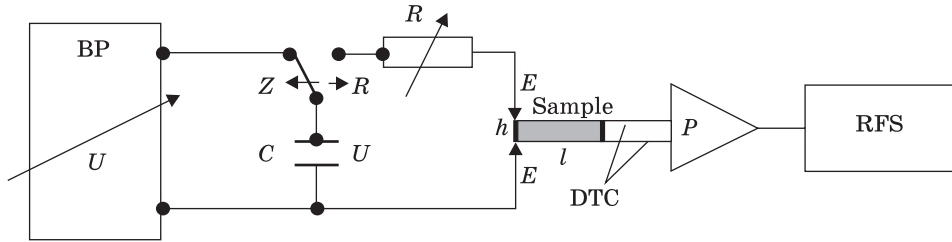
Fig. 9. Scheme of the implementation of the method: BP — adjustable power supply, R — additional resistor, DTC — differential thermocouple, C — electric capacitance, E — discharge electrodes, $Z{\leftrightarrow}R$ — 'charge–discharge' switch, P — signal amplifier, RFS — waveform and time recorder $t_{1/2}$ [44]

excitation of the thermal pulse is preliminarily selected, and the previous value of the duration t of the discharge pulse is determined from the criterion [27].

From the power supply unit and through the switch '$Z \leftrightarrow R$', initially in the 'C' position, the electric capacitance C is charged to a predetermined voltage value U, after which the switch '$Z \leftrightarrow R$' is transferred to the 'P' position and the capacitance C is discharged through an additional resistor R, electrodes E and one of the sides in width h of a rectangular film sample of length l. A signal was taken through a differential thermocouple (DTC), consisting of chromel and alumel conductors connected at a distance h from each other to the opposite side of the film sample, and sent through an amplifier P to the RFS recorder, with which the time $t_{1/2}$ was recorded.

An iron film 0.5 μm thick was used as a sample, which was deposited by electrovacuum sputtering through a 2×5 mm mask on a dielectric substrate made of glass-ceramic ST32-1. The variable resistor R allows smooth adjust the duration t_{p} of the discharge, which can be determined by the formula $t_{\mathrm{p}} = (4-5)R_{\Sigma}C$, where R_{Σ} consists of the resistance R and the resistance of the section $h = 2$ mm of the sample with the investigated specific resistance ρ of the material. The capacitance C was chosen from the calculation of the discharge energy $E = CU^2/2$, which should not exceed the critical energy that can lead to electroerosive destruction of the sample along the length of the side of the sample h, through which the electric capacitance C is discharged.

From relation (30), the required discharge energy E was determined and, in the case of an electric discharge, for example, using a capacitor with a capacitance C, by including an additional resistor R in the discharge circuit, the value $t = RC$ is provided, and the discharge energy is provided by charging it before the voltage U. The length r of the film or foil, the thermophysical characteristics of which are chosen, is estimated from the ratio $r \propto 2\sqrt{at}$. Discharge of the capacitor provides

excitation of a thermal pulse on the area s of one of the ends of a rectangular film or foil of width b and length r, registration at the opposite end of the film or foil of the time to reach half the value of the maximum temperature ($t_{1/2}$), determination of thermophysical characteristics according to already known formulas.

The thermophysical characteristics of the 1 µm thick film made of U12 carbon steel by vacuum sputtering of a target onto a nonconductive ST2-1 glass-ceramic substrate. Based on the main component of steel (iron), we chose the values of $k = 70$ W/(°C·m), $\rho = 7.8 \cdot 10^{-3}$ kg/cm³, $T_{melt} = 1535$ °C, $a = 0.22$ cm²/s and an area $s = 0.56 \cdot 10^{-8}$ m² of a rectangular film with a narrow side $h = 0.2$ mm, on which the capacitor was discharged. From the criterion [27], the approximate duration of the discharge was determined, which is $t = 0.25 \cdot 10^{-3}$ s, and from here and from (19), the maximum critical energy of the discharge J. At a voltage of $U = 5$ V, which is the most common standard in computing and measuring equipment, we can calculate the value $C = 2E/U^2 \approx 80$ µF and $R = t/C \approx 3.1$ Ohm.

The discharge of a capacitor $C = 80$ µF charged to a voltage $U = 5$ V was carried out through a resistor $R = 3.1$ Ohm and an area $s = 0.56 \cdot 10^{-8}$ m² of a rectangular film with a narrow side $b = 0.2$ mm and temperature (T_m) at the opposite end of the film $r = 2$ mm. Time $t_{1/2}$ was of 0.047 ± 0.001 s at $T_{max} = 10.2 \pm 0.1$ °C. Thus, $a = 1.2 \cdot 10^{-5}$ m²/s. This value was used to refine the duration of the discharge t, which was $t = 0.47 \cdot 10^{-3}$ s.

Since an increase in the value of capacitance C in accordance with (30) will lead to an undesirable increase in the critical value of the energy E of the discharge, t was corrected by changing R, the calculation of which gives $R = 6$ Ohms.

Further calculation of the remaining thermophysical parameters does not differ fundamentally from the calculations of these quantities by the laser-flash method; therefore, it is not presented.

3.1.3. Implementation of the Parker's Method and Differential Method Based on It

The practical implementation of the Parker's method consists of the formation of a thermal pulse at one of the ends of a cylindrical flat sample and the registration of temperature changes on the opposite surface with subsequent processing.

The scheme for determining the TRC with one-sided measurement of the sample temperature is shown in Fig. 10.

The introduction of corrections for heat losses by the calculation method is not without drawbacks. This is due to the need for a chain of introduced assumptions and the uncertainty of the properties of many
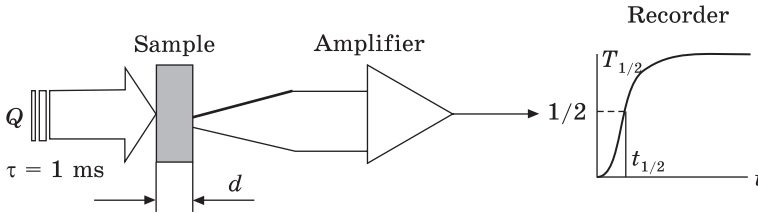
Fig. 10. Scheme for measuring the thermophysical properties of bulk materials using the Parker method [8]

materials at high temperatures (in particular, the emissivity to take into account radiant heat transfer). In this regard, a method has been proposed that makes it possible to measure the desired parameters in the time range, when the influence of heat transfer does not yet distort the shape of the temperature response. The differential method is based on a predetermined temperature ratio on the front and back surfaces of the sample.

The temperature distribution in a flat infinite plate of thickness L, on one of the surfaces of which ($x = 0$) a flat pulsed-heat source acts, is described by the equation [3, 52]:

$$T(x,t) = T_{\max}\left[1 + 2\sum_{n=1}^{\infty}\frac{\cos n\pi x}{L}\exp\left(-\frac{n^2\pi^2}{L^2}a\tau\right)\right], \qquad (34)$$

where x is current co-ordinate from 0 to L; τ is time [s]; a is the coefficient of thermal diffusivity [m^2/s].

Calculated relation for the thermal diffusivity coefficient [52] is

$$a = \frac{\omega_0 L^2}{\pi^2 \tau_{2.97}}, \qquad (35)$$

where (35) is the moment of time, when the ratio of temperatures on opposite surfaces of the sample, as a result of a thermal pulse, is equal to [53]

$$\frac{T(0, \tau_{2.97})}{T(L, \tau_{2.97})} = \frac{Q_0(\omega_0)}{Q_L(\omega_0)} = 2.97, \qquad (36)$$

The specific heat capacity [J/(kg·K)] of a material is defined as [52]

$$C_p = \frac{q}{\rho^2 L T_{\max}}, \qquad (37)$$

where ρ is the density of the material [kg/m^3], q is the specific energy of the thermal pulse [J/m^2].

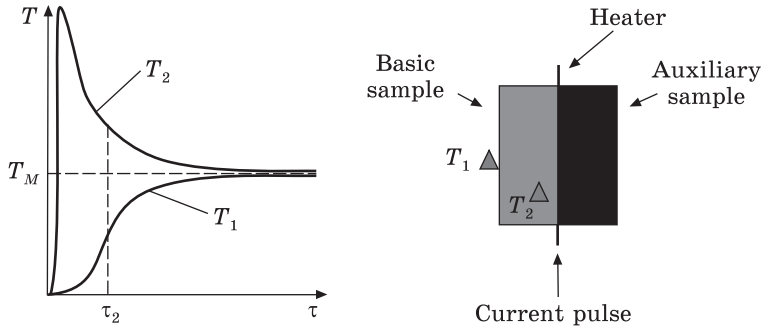Then, the calculated ratio for thermal conductivity ($k = aC_p$) will be written as [52]

Fig. 11. Graph of temperature change on the back irradiated surface of the sample (T_2) and scheme for measuring thermophysical characteristics in the differential version (T_1) of the method [53]

$$k = \frac{1.386q}{\pi^2 L \Delta T \tau_{2.97}} \,.$$

(38)

The scheme for measuring TRC with two-sided temperature measurement (differential method) is shown in Fig. 11 [53].

3.1.4. Determination of the Transverse Thermal Conductivity of Aluminium–Nickel Films by the 3ω Method

To remove heat from powerful electronic devices [54, 55] and IR-filters [56, 58], it is necessary to use highly thermally conductive insulating thin films or coatings. Monocrystalline AlN is one of the promising materials for efficient heat conductors in microelectronics devices due to its high thermal conductivity coefficient at room temperature ($k = 320$ W/(m·K)) [59] and is over 170 W/(m·K) for pseudo-single-crystalline layers [7]. However, the thermal conductivity of thin films can differ significantly from their massive counterparts [60–66]. Thin films obtained using vacuum deposition technologies contain many impurities, dislocations, and grain boundaries, where electrons and phonons are scattered, that leads to a decrease in thermal conductivity of the films [7, 62, 65, 66]. These factors have different effects on heat transfer in the plane and perpendicular to the plane of the film that leads to anisotropic thermal conductivity of thin films. Thermal conductivity of polycrystalline AlN films depends on the growth procedure, thickness, type and density of defects, oxygen content and the overall quality of the crystalline structure. For AlN films obtained by magnetron sputtering in different modes on silicon substrates, the values of thermal conductivity coefficient are measured to be at room temperature in the range between 0.8 and 130 W/(m·K) [62] or between 2 and 170 W/(m·K) [66].

Therefore, the accurate measurement of thermal conductivity in the plane $(k_\parallel)$ and in the direction perpendicular $(k_\perp)$ to the plane of polycrystalline thin films, in particular, AlN, is critically necessary for the design and creation of microelectronic devices.

The paper [67] investigates the transverse component of the thermal conductivity $(k_\perp)$ of AlN films with a thickness of 1–3 µm, which were deposited on a monocrystalline silicon substrate of 20×8×0.45 mm or on an aluminium substrate of 20×30×2 mm. The AlN films were synthesized in vacuum technological equipment having a hybrid helicon-arc ion-plasma reactor [68−70], which includes a helicon plasma source [71, 72] and plasma-arc accelerators [73] combined in one process chamber. The equipment provides unique technological characteristics, in particular, low operating temperatures (30−300) °C on the substrate as well as the formation of a working gas ions flow from a helicon source with a density of 5−10 mA/cm² in the substrate area and energies up to 100−150 eV. At the same time, the vacuum-arc source generates accelerated plasma flow of a consumable cathode material with a density of 10−20 mA/cm² and ion energies up to 100−150 eV.

An Al film with a thickness of 0.03−0.1 µm was deposited on the AlN film surface in a single technological cycle (*in situ*) [67]. A heater tape of 280×70 µm was formed from an Al film by photolithography on AlN films deposited on Si substrates or a tape of 280×35 µm by means of the deposition on AlN films on Al substrates. As can be seen, the smaller Al width of the heater strip *2b* was of 35 µm that is much larger than the thickness of the studied AlN film, which was of 1−3 µm. Thus, the conditions (21) for a one-dimensional heat flux in the perpendicular to the plane of the AlN films were satisfied [7].

Further, to determine the thermal conductivity coefficient $k_\perp$ of AlN films according to formula (20), it is necessary to determine the temperature coefficient of resistance (TRC) α of the Al heater tape. The measurement of the resistance of the Al heater tape at different temperatures was carried out by the four-probe method on an information-measuring complex [74]. The manipulator with the sample was placed in a heating cabinet, and the *I−V* characteristics of the samples were measured at different temperatures. Based on the obtained experimental *I−V* characteristics, the temperature coefficient of resistance α of the Al heater films was calculated as

$$\alpha = \frac{1}{R}\left(\frac{dR}{dT}\right). \tag{39}$$

The resistance of the Al heater tape of 280×70 µm was $R_0 = 127$ Ohm. In this case, the resistance of the part of the tape, on which the Joule heating occurred, according to the calculation was of $0.64R_0$. Electrical resistance of this Al heater tape at 19 °C was of 90.7 Ohms and, at
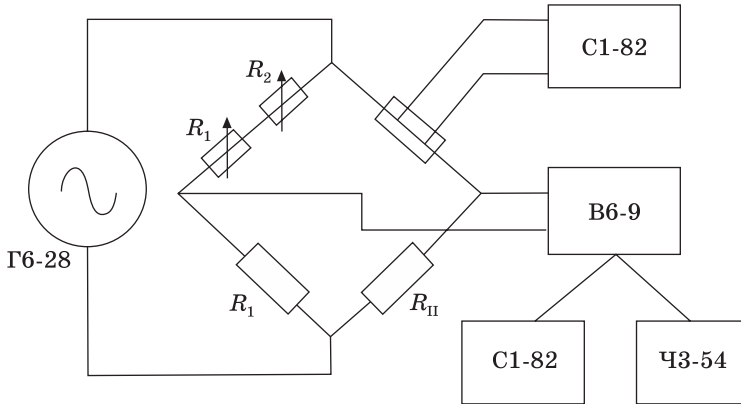
Fig. 12. Block diagram of an equipment for changing the thermal conductivity of AlN thin films (R_1, R_2 are precision resistors for coarse and fine balancing of the bridge) [67]

99 °C, 94.2 Ohms. The calculation gave the value of the temperature coefficient of resistance $\alpha = 0.48 \cdot 10^{-3} \cdot K^{-1}$ [67].

The measurement of the unbalance voltage at the third harmonic $W_{3\omega}$ was made using a Winston bridge, setting the alternating current frequencies ω with a generator in the range of $f = \omega/2\pi = 20-30.000$ Hz [67]. The block diagram of the equipment used to measure the thermal conductivity $k_\perp$ of AlN thin films is shown in Fig. 12. In the experimental equipment for determining the thermal conductivity coefficient $k_\perp$ of thin films, the following instrumentation was used: *1* — signal generator G6-28 (Г6-28); *6* — selective microvoltmeter V6-9 (В6-9), at the output of which the parameters of the signal at the third harmonic were recorded by an oscilloscope S1-82 (C1-82) and a frequency meter Ch3-54 (Ч3-54).

First (at small generator signal values with a frequency $f = \omega/2\pi$), the Winston bridge arms are being balanced to obtain the voltage $W_\omega = 0$ on the bridge diagonal. Next (at operating values of the generator signal with frequency $f = \omega/2\pi$), the voltage of unbalancing on the bridge diagonal at the third harmonic $W_{3\omega}$ is being measured. The value of $W_{3\omega}$ is fixed after its stabilization, which indicates the establishment of thermal balance in the system containing the heater, the investigated film, and the substrate. Similarly, measurements of $W_{3\omega}$ are carried out at other frequencies.

Measurement of the output unbalance voltage of the third harmonic $W_{3\omega}$ on the Winston bridge diagonal gave such a dependence on the double frequency 2ω (Fig. 13) at the bridge shoulders $R_I = R_{II} = 10$ Ohm. As we can see, the dependence $W_{3\omega} = f(2\omega)$ is well approximated by a straight line on a semi-logarithmic scale at four orders of magnitude of frequency change 2ω. Drop $\Delta W_{3\omega} = 38$ μV with drop $\Delta\ln 2\omega = 9.21$.
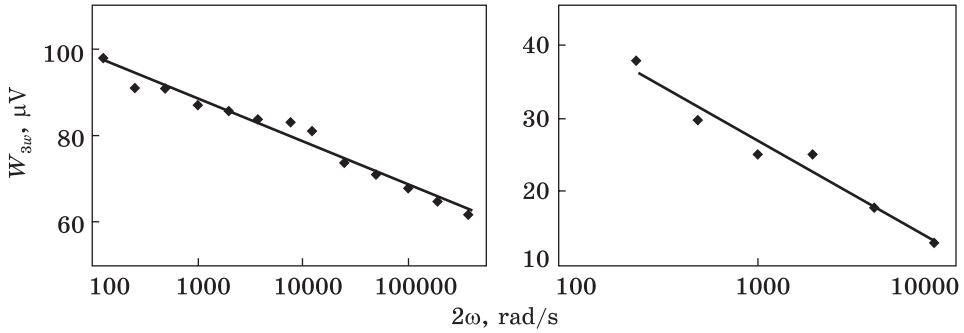
Fig. 13. Dependence of the output voltage of the third harmonic $W_{3\omega}$ on the Winston bridge diagonal on the double frequency 2ω for the AlN film on monocrystalline Si substrates [67]

Fig. 14 Dependence of the output voltage of the third harmonic $W_{3\omega}$ on the Winston bridge diagonal on the double frequency 2ω for the AlN film on the Al substrate [67]

According to Kirchhoff's rules, we determine the voltage drop of the third harmonic $U_{3\omega}$ on the Al heater tape of the experimental sample (Fig. 12):

$$U_{3\omega} = \frac{W_{3\omega}(R_0 + R_{\text{II}})}{R_{\text{II}}} = 13.7 W_{3\omega}, \tag{40}$$

where R_0 and R_{II} are the resistances of the Al heater tape of the sample and the shoulder of the bridge, respectively.

The peak amplitude of the voltage across the Al heater tape was $U_0 = 1.4$ V. Let us calculate the coefficient of thermal conductivity $k_{\perp\text{AlN-Si}}$ of the AlN film on the Si substrate using the formula (20). Let us calculate

$$\frac{\partial \ln(2\omega)}{\partial U_{3\omega}} = \frac{\Delta \ln 2\omega}{\Delta U 3\omega} = 9.21/13.7\Delta W_{3\omega} = 1.8 \cdot 10^4;$$

then, the transverse thermal conductivity $k_{\perp\text{AlN-Si}}$ of the AlN film on the Si substrate will be

$$k_{\perp\text{AlN-Si}} = \left[\frac{U_0^3}{4\pi l \cdot 0,64 R_{22C}}\right] \frac{\alpha \partial \ln(2\omega)}{\partial U_{3\omega}} = 82.9 \text{ W/(m·K)}.$$

The obtained value $k_{\perp\text{AlN-Si}}$ is consistent with the literature data [62, 66].

Similarly, for the AlN films on the Al substrate, based on experimental data (Fig. 14), we will calculate the thermal conductivity coefficient $k_{\perp\text{AlN-Al}}$ [67]:

$$k_{\perp\text{AlN-Si}} = 45.8 \text{ W/(m · K)}$$

that is the highest value among those known for Al metal substrates, which are widely used for cooling LED devices [75].

### 3.2. Thermal Probing of Layered Structures

The technique is based on the principle of recording the features of the passage of a thermal pulse through a multilayer system having layers with different thermal conductivity k_i. As known, the coefficient of thermal conductivity of a solid body is inversely proportional to the thermal resistance $W \propto k - 1$. In such systems under study, the total thermal resistance W_Σ consists of individual thermal resistances W_i and each of the layers and interlayers between them W_p [77]:

$$W_\Sigma = \Sigma(W_p + W).\tag{41}$$

The method was based on the so-called express method by Parker [8] for measuring thermophysical characteristics: temperature, thermal conductivity, and heat capacity. This method, which has been modernized for the characterization of films, has shown itself well in studies of pure materials and their compounds in a wide temperature range [9].

The effectiveness of the approach to determining the thermal inertia time depending on the structural state of a substance using the Parker's method [8] was experimentally verified in [27]. Such an approach can become effective when there is transmitting a thermal pulse (TP) introduced into a layered structure by using a pulsed laser.

General schemes for studying and evaluating the thermal resistance of layered and multilayer systems with different thermal and electrical conductivity of the layers are shown in the corresponding figures (Fig. 15, *a*, *b*).
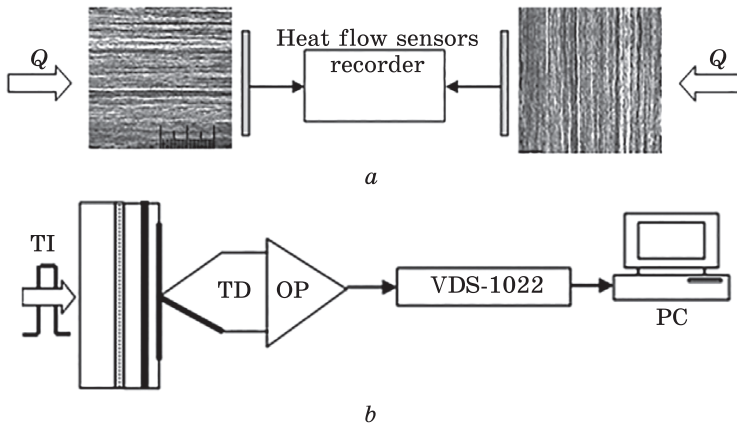
Fig. 15. The general scheme for studying layered structures (*a*) and the block diagram for studying multilayer systems with different thermal and electrical conductivity of the layers (*b*): TI is a thermal impulse (*Q*), TD is a heat flow sensor (in particular, a thermocouple), OP is an operating amplifier, VDS-1022 (registrar) — digital oscilloscope attachment to a computer (PC) [77]
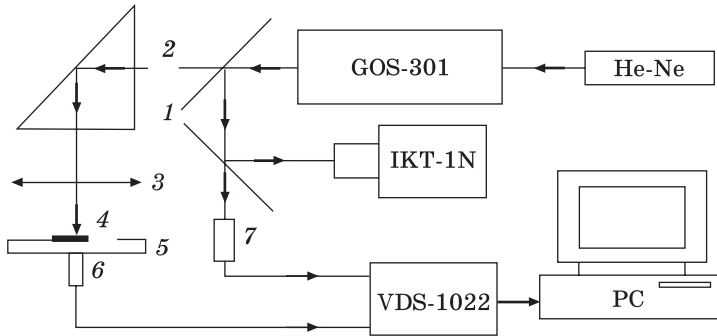
Fig. 16. Optoelectronic scheme of thermal probing of a multilayer system for estimating the integral thermal resistance, excited by a laser (GOS-301) pulse in a quasi-stationary mode ($\tau_i = 1$ ms). Here, *1* — light-separating plates for monitoring the characteristics (τ_i and q_i) of the laser beam, *2* — return prism *3* — focusing optics, *4* — a metal film on the substrate *5*, *6* — infrared receiver (MLX90614), *7* — coaxial photocell (FK-2), GOS-301 — solid-state pulsed laser, He–Ne — low-power gas laser ($\lambda = 0.6328$ μm) for adjusting the optical system and providing targeted irradiation of films, IKT-1N — laser pulse energy *Q* meter, VDS-1022 — digital storage two-channel oscilloscope attachment to a PC for simultaneous recording of the parameters of a laser pulse and a thermal response pulse of a multilayer system [77]

The W_Σ value for ensuring the invariance of the layer resistances W_p will mean an increase in W_i due to the degraded quality (roughness) of the interface. This can be determined only in a comparative experiment with probing two multilayer systems with a thermal pulse, one of which would be perfect in advance.

Using a similar technique, it is proposed to evaluate the adhesive properties of films and coatings on products. Based on the described method concerning thermophysical measurements of bulk materials [40, 41], a method was developed for measuring the thermophysical characteristics of films and foils. A block diagram of the installation based on the Parker's method is shown in Fig. 16.

The developed ideology is implemented using the Arduino hardware-computing platform. To measure the temperature, an MLX90614 non-contact temperature meter module was used. It is designed for non-contact measurement of the absolute temperature of objects. Temperature measurement range was from -70 to $+380$ °C, measurement accuracy was of 0.5 °C for the range from 0 to $+50$ °C, resolution was of 0.02 °C. Appropriate software has been developed to record the measured temperature of an object over time.

### 3.2.1. Measurement of Adhesion and Thermal Resistance of Film Systems

Approbation of the possibility of the method was carried out when assessing the quality of adhesion carried out on Fe films, which were deposited on a polycor substrate by electron-beam sputtering in a vacuum. The films were deposited simultaneously because of the corresponding masks, which had the same holes, under one of which the substrate was thoroughly cleaned, and under the second one, it remained uncleaned, which should have previously worsened the adhesion of the film obtained in this place to the substrate.

The films on the substrate were irradiated with a laser pulse in a quasi-stationary mode ($\tau_i = 10^{-3}$ s), at which no additional structural changes occurred in the interface zone. This ensured the excitation of a probing thermal pulse perpendicular to the interface plane. The passage of a thermal pulse was recorded from the reverse side of the substrate, registering infrared radiation with an MLX90614 sensor (Fig. 16). As a result of the approbation, a noticeable attenuation of the signal was detected after passing the heat flux through the system with a Fe film deposited on an uncleaned polycor substrate in comparison with the signal after passing through the system with a thoroughly cleaned substrate. Thus, it was possible to feel the creation of thermal resistance by impurities in the 'film–uncleaned substrate' interface.

The method was tested on multilayer systems with different layer conductivity. The studied structures were Al and Cu/AlN/Al multilayer systems. An Al sample was used to test the sensitivity of the developed setup to conditions at the interface between two materials. For this, in the first case, an aluminium sample was used, which was located at a certain distance from the film of the inlet of the temperature meter. In the second case, the aluminium sample was brought into contact with the inlet film, which was coated with thermal paste to provide improved thermal contact.

Another system tested was the Cu/AlN/Al multilayer structure shown in Fig. 17.

The results of the performed measurements are shown in Fig. 18, showing the dependence of the temperature T on the reverse surface of the Al sample, and in Fig. 15 for Cu/AlN/Al multilayer sample *versus* time.
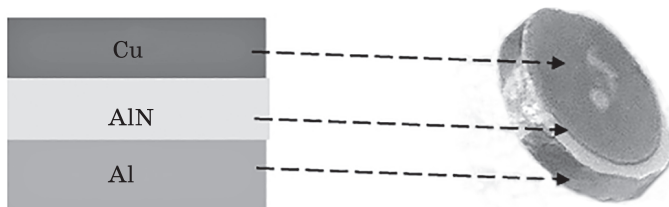
Fig. 17. Scheme (left) and external view (right) of a sample with a Cu/AlN/Al heterostructure

Fig. 18. Dependence of the measured temperature T on the reverse surface of the Al sample on time t, where *1* — sample without thermal paste, *2* — with thermal paste
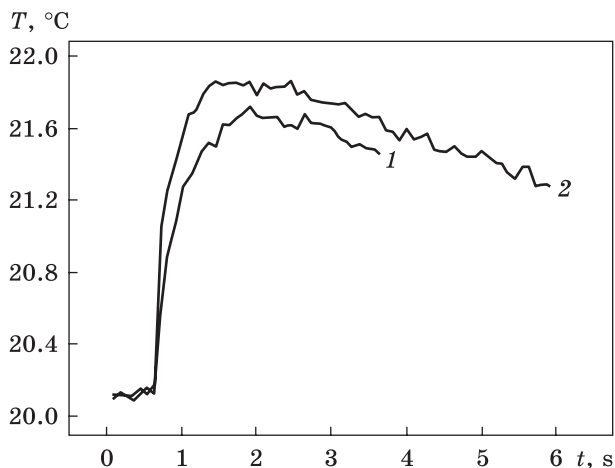
As can be seen from Fig. 18, when providing thermal contact using thermal paste, a higher rate dT/dt of heat transfer for the absorption of an energy pulse is observed in comparison with the data obtained without the use of thermal paste. In fact, this correlates with the results obtained in the study of the effect of the quality of adhesion of iron films to polycor substrates described earlier. This indicates that the sensitivity of the developed method to the state of interfaces, which play a significant role in heat transfer in multilayer structures, is acceptable.

3.2.2. Irreversible Heat Transfer in the Cu/AlN/Al System

In the case of a change in the direction of the heat flow through the Cu/AlN/Al multilayer system, a difference in temperature measurements of the opposite sample surface irradiated by the laser is observed (Fig. 19). There is a noticeable difference in the temperature readings during the passage of a probing thermal pulse through the system from Cu to Al through the AlN layer and *vice versa*. Since the reflection coefficients of aluminium and copper are almost the same (0.90 and 0.93, respectively) for the radiation used with a wavelength of 1.06 μm, the difference in absorbed energy can be neglected. When processing the results of the experiment, the difference in the emissivity of aluminium and copper was taken into account, and it is believed that heating by 1–2 degrees does not change it. The review [78] considers possible explanations for such an irreversible heat flow due to roughness on the contact surface, due to a change in the average contact temperature due to a change in temperatures at the outer boundaries of the system and the corresponding different change in the thermal conductivity coefficients of the layers, a change in the contact area due to different coefficients of linear expansion. However, it is also necessary to take into account the peculiarities of thermal momentum transfer during electron–phonon interaction. This interaction plays a significant role in the transfer of a thermal impulse from a metal layer (Al or Cu) to a dielec-
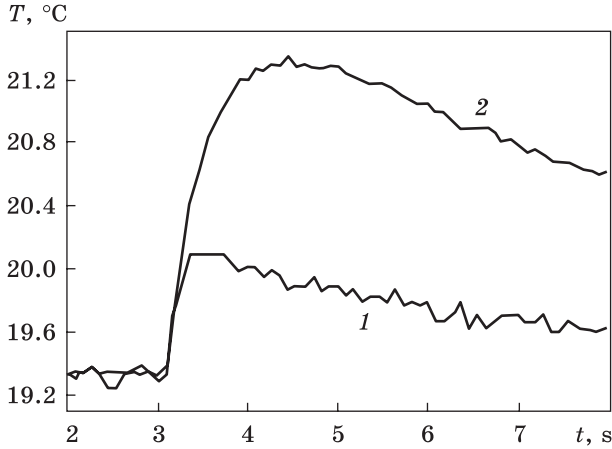
Fig. 19. Dependence of the measured temperature T on the reverse surface of the Cu/AlN/Al multilayer sample on time t and the direction of heat flow, where *1* — Cu/AlN/Al, *2* — Al/AlN/Cu

tric (AlN) and from a dielectric to a metal layer (Cu or Al). Such an interaction is determined by the ratio of the Debye temperatures of these materials [79]. For example, it can be expected that, when a pulse is transferred from a dielectric with high T_D, high-energy phonons are first absorbed by the electron subsystem of the metal and then converted into phonons. This is the scheme of thermal-impulse transfer at the boundary of two layers, which can explain the irreversible effect in the heat transfer of the Cu/AlN/Al system that is observed in Fig. 19. It makes clear that the sequence of layers along the path of a thermal pulse affects the efficiency of heat transfer during its passage.

It is shown that the Parker's method for determining thermal conductivity makes it possible to investigate not only the adhesive properties of the coating system (the base), but also the thermal resistance of multilayer structures. The sensitivity of the method is sufficient to reveal the irreversibility of thermal resistance in such systems.

3.3. Study of the Thermal Properties of Film Materials by the Point Heating Method

Regarding the prospects for the development of methods for characterizing the thermal properties of materials and, in particular, film ones, one can consider the method of point heating [80]. The theoretical foundations of this method were laid in the works [52, 76], where the authors solved the Fourier equation for heating a semi-infinite solid.

The authors of Ref. [80] showed that the results obtained in Refs. [52, 76] can be applied to study the thermal conductivity of thin films in time intervals when the experimental graphs are linear, according to the theory, and do not experience thermal reflection of the heat flux from the opposite interface of the substrate. The experimental results obtained in Ref. [80] correlate well with the experimental results of

other aut-hors who used a complex expe-rimental technique.

The principle of the point heating method [80–82] for measuring the ther-mal conductivity ($k_\perp$) and thermal diffu-sivity (a) of thin materials is based on three relationships between the increase in the temperature of the sample surface being heated by a heat source and the thermophysical properties of the sample. These ratios are obtained by solving the Fourier equation in different time ran-

Fig. 20. Scheme for solving the Fourier equation [76]

ges. Temperature rise measured over a short time range is proportional to the square root of time. The slope of this straight line gives the value $k_\perp/a^{1/2}$. In addition, the rise in tem-perature over a long period of time is inversely proportional to the square root of time. The slope of this line gives the value $a^{1/2}$, and the point of intersection at $1/t^{1/2} = 0$ gives $k_\perp$. Therefore, thermal conducti-vity and thermal diffusivity can be determined using two relationships of the above three relationships.

As shown in Fig. 20, a sample where $z \geq 0$ is heated uniformly by a circle of radius r.

It is further assumed that heat is dissipated only into the sample. The solution of the Fourier equation under these conditions is due to Ref. [76]. The temperature rise ΔT at position $x = y = z = 0$ is written as an equation [76]

$$\frac{k_\perp}{a^{1/2}} = \left(\frac{2Q / \pi^{3/2} r^2}{d\Delta T / d(t^{1/2})} \right), \tag{42}$$

$$\Delta T = (Q/\pi r k_\perp)\tau\{\pi^{-1/2} - \mathrm{ierfc}(1/\tau)\}_i^{ex}. \tag{43}$$

Here, Q is the amount of heat input per unit time, the dimensionless number $\tau = 2(at)^{1/2}/r$, $\mathrm{ierfc}(x) = \exp(-x^2)/\pi^{1/2} - x\mathrm{erfc}(x)$. Then,

$$\Delta T = (Q/\pi r k_\perp)f(\tau), \tag{44}$$

$$f(\tau) = \{\pi^{-1/2} - \mathrm{ierfc}(1/\tau)\}. \tag{45}$$

Here, $f(\tau)$ simplifies depending on the range of τ. Therefore,

$$\tau < 0.7, \quad f(\tau) = \pi^{-1/2}\tau; \tag{46}$$

$$\tau \geq 1.0, \quad f(\tau) = 1 - (1 - \pi^{-1/2})/\tau = 1 - 0.4358/\tau. \tag{47}$$

Comparison of the exact value of $f(\tau)$ with the value of the approxi-mate expression according to Eqs. (46) and (47) is shown in Figs. 21 and 22.
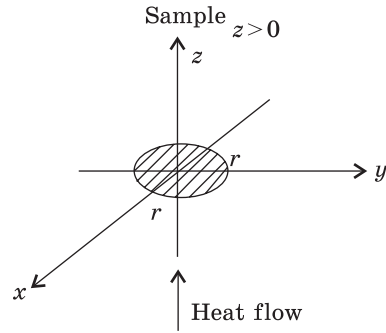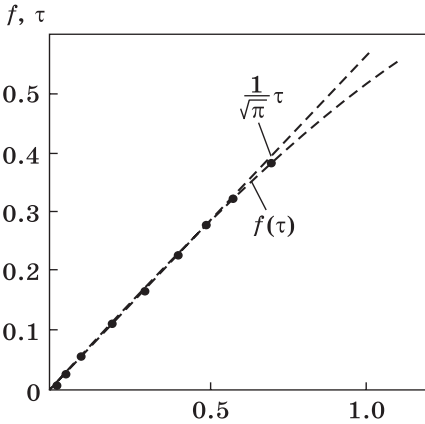
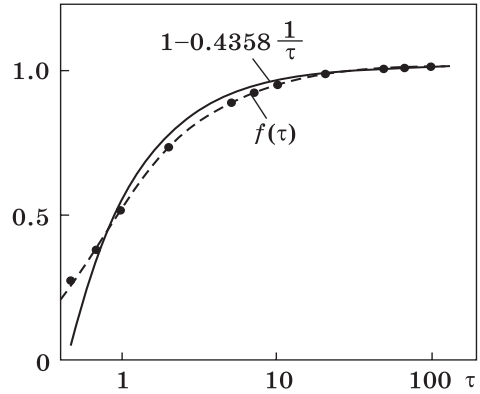*Fig. 21.* Relationship between $f(\tau)$, $\pi^{-1/2}\tau$, and τ [76]

Fig. 22. Relationship between $f(\tau)$ or $(1 - 0.4358/\tau)$ and τ [76]

From Figs. 21 and 22, it can be seen that the value of $f(\tau)$ has an error of 3% or less when $\tau \leq 0.7$, and when $\tau \geq 1$, it can be approximated by a simple function with an error of 10% or less.

From Eqs. (41) and (42) after differentiation of ΔT with respect to $t^{1/2}$, the value of $k_{\perp}/a^{1/2}$ is determined by the following equation:

$$k_{\perp}/a^{1/2} = \frac{2Q/\pi^{3/2}r^2}{d\Delta T/d(t^{1/2})} \quad . \tag{48}$$

That is, $k_{\perp}/a^{1/2}$ is the reciprocal of the temperature increase ΔT and the square root of time t and can be determined from the slope of the straight line.

From Eqs. (44) and (47), we can obtain the equation for $k/a^{1/2}$ when $\tau \geq 1$:

$$k_{\perp}/a^{1/2} = \frac{-0.2179(Q/\pi)}{d\Delta T/d(1/t^{1/2})} . \tag{49}$$

From Eqs. (44) and (47) at $t = \infty$, we obtain

$$k_{\perp} = \frac{Q}{\pi r \Delta T(\infty)} . \tag{50}$$

The thermal conductivity k and thermal diffusivity a of thin AlN films were determined based on the obtained experimental data.

Figure 23 shows the scheme for measuring the temperature of a thin AlN film, the thickness of which was of 3 μm. A heat flux q was supplied to the film through a circular section of 5 mm in diameter, which was created by a 3 W warm white LED, when an electric current was passed through it. The temperature at the top of the film was measured with a thermistor. It is known that the thermal conductivity of
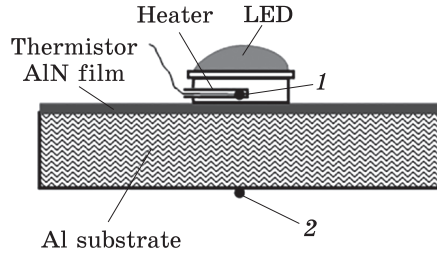
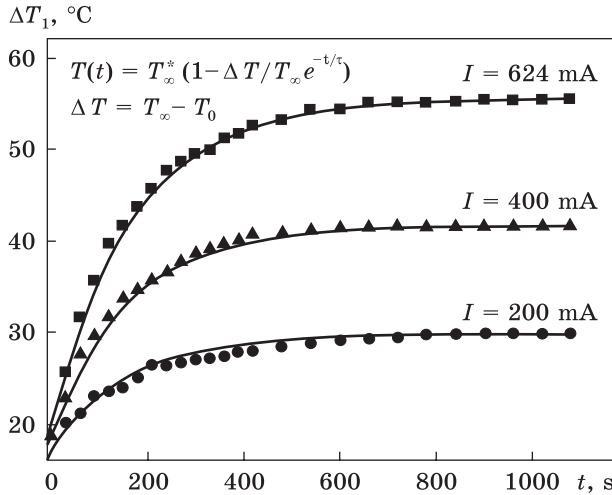*Fig. 23.* Scheme of heating the test sample: *1* and *2* are points (places) of the temperature measuring

Fig. 24. Temperature dependence of the heating of the surface of the AlN/Al sample by current of different magnitudes
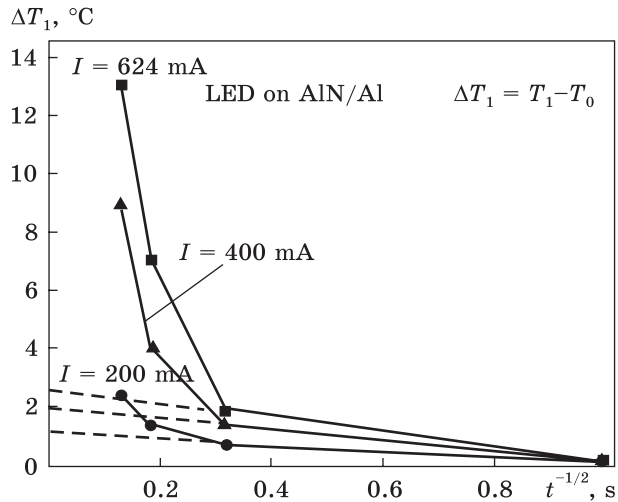
$$T(t) = T_\infty^* (1 - \Delta T / T_\infty e^{-t/\tau})$$
$$\Delta T = T_\infty - T_0$$

$I = 624$ mA

$I = 400$ mA

$I = 200$ mA

Fig. 25. The nature of the temperature rise in a long range of measurement time of the AlN film

$I = 624$ mA

LED on AlN/Al $\Delta T_1 = T_1 - T_0$

$I = 400$ mA

$I = 200$ mA

thin anisotropic films [81]. If the dimensions of the heater are larger than the film thickness; then, the practically entire heat flux is directed across the film, and in this case, the transverse thermal conductivity of

the thin film is measured. The research sample consisted of an AlN film, which was condensed onto a metal substrate of 1.5–2 mm thick. Figure 23 shows the scheme of heating the test sample.

To create a heat flux through the sample, a heat flux source consisting of a high-power LED (3 W warm white) mounted on a copper cylinder of 5 mm in diameter and of 3 mm high was glued to it using KPT-19 thermal paste. The cylinder had a hole, into which a thermometer was inserted. The thermometer readings were related to the temperature T_1 of point 1. The temperature T_2 was measured with a thermometer on the bottom surface of the sample at point 2. The experimental dependence of the temperature T_1 of heating the upper surface of the sample on the heating time is shown in Fig. 24.

From the dependence of T_1 on t for different load currents, the dependences of the temperature increase $\Delta T_1 = T_1 - T_0$ on $t^{-1/2}$ were plotted (Fig. 25).

As you can see, for all currents, the graphs have straight sections. The deviation from the linear dependence occurs for all currents for about 10 seconds. Extrapolating straight sections to the section with axis ΔT_1, we obtained for current $I_1 = 200$ mA the value $\Delta T_1(t = \infty) = 1.2$ °C, for current $I_2 = 400$ mA the value $\Delta T_1(t = \infty) = 2$ °C, and for $I_1 = 600$ mA $\Delta T_1(t = \infty) = 2.7$ °C. As seen, the temperature $T_0 + \Delta T_1(t = \infty)$ turned out to be less than $T_{1\infty}$.

From Eq. (50) and the obtained values of $\Delta T_1(t = \infty)$, the transverse thermal conductivity was determined for different heating currents. The amount of heat Q supplied per unit time from the heat flux source to the sample surface at different load currents was $Q_{200} = 0.43$ J/s, $Q_{400} = 0.93$ J/s, and $Q_{600} = 1.47$ J/s. Thus, the transverse thermal conductivity was also calculated: $k_{\perp 200} = 45.6$ W/(m·K), $k_{\perp 400} = 59.2$ W/(m·K) and $k_{\perp 600} = 69.3$ W/(m·K).

The obtained values correspond to known results of other authors. According to work [81], for AlN films synthesized by RF reactive magnetron sputtering on Si substrates of 1000 nm thick, $k_\perp = 14.9$ W/(m·K) was obtained with a theoretical estimate of 114 W/(m·K). The authors of Ref. [82] fabricated the AlN films by reactive magnetron sputtering on the Si substrates. It was found that the thermal conductivity of films in the transverse plane increases from 60 to 90 W/(m·K) with an increase in thickness from 1 to 2 μm.

4. Conclusions

When analysing a number of well-known methods for characterizing the thermal properties of a solid body, the most effective studies of multilayer systems were determined.

Based on Parker's express method for determining the thermophysical characteristics of flat objects, a technique has been developed and

tested for estimating the integral thermal resistance of a multilayer system. The tests carried out showed the ability of the method to affect the thermal resistance of the system, both its components and the state at the interfaces.

The effect of irreversibility in the heat transfer of the Cu/AlN/Al system is revealed. This effect is explained by the features of heat transfer processes at the metal−dielectric interface depending on their Debye temperatures and taking into account the electron−phonon interaction.

The modification of the 3ω method makes it possible to determine the thermal conductivity of thin films, both in the plane $k_\parallel$ and across the plane $k_\perp$, by changing the heater width. The point heating method is suitable for studying thermal processes in microelectronic elements.

REFERENCES

1. Charles Kittel, *Introduction to Solid State Physics* (John Wiley & Sons: 2005).
2. L.N. Larikov and Yu.F. Yurchenko, *Struktura i Svoistva Metallov i Splavov* [Structure and Properties of Metals and Alloys Directory] (Kiev: Naukova Dumka: 1985), p. 438 (in Russian).
3. H. Carslaw and J. Jaeger, *Conduction of Heat in Solids* (New York: Oxford University Press: 1959).
4. T. Borca-Tasciuc, A.R. Kumar, and G. Chen, *Rev. Sci. Instrum.*, **72**: 2139 (2001);
   https://doi.org/10.1063/1.1353189
5. D.G. Cahill, *Rev. Sci. Instrum.*, **61**: 802 (1990);
   https://doi.org/10.1063/1.1141498
6. David de Koninck, Thermal Conductivity Measurements Using the 3 Omega Technique: Application to Power Harvesting Microsystems (*Department of Mechanical Engineering McGill University Montréal*, *Canada: 2008*), p. 106.
7. M. Bogner, G. Benstetter, and Y.Q. Fu, *Surf. Coat. Technol.*, 320: 91 (2017); https://doi.org/10.1016/j.surfcoat.2017.01.100
8. W.J. Parker, R.J. Jenkins, C.P. Butler, and G.L. Abbott, *J. Appl. Phys.*, **32**: 1679 (1961);
   https://doi.org/10.1063/1.1728417
9. M.E. Gurevich and A.E. Pogorelov, Primeneniye Lazernoy Tekhniki dlya Teplofizicheskikh Issledovaniy [Application of Laser Technology for Thermophysical Research, *Physical Methods for the Study of Metals* (Kiev: Naukova Dumka: 1981), p. 3−23 (in Russian).
10. R.E. Taylor and J.A. Cape, *Appl. Phys. Letters*, **5**: 212 (1964).
11. R.E. Taylor, J. Jortner, and H. Groot, *Carbon*, **23**, No. 2: 215 (1985).
12. K. Etori, *Japan. J. Appl. Phys.*, **8**, No. 11: 1357 (1969).
13. K. Etori, *Bull. Fac. Eng. Miyazaki Univ.*, No. 16: 70 (1969).

14. Susumu Namba, Pil Hyon Kim, and Tsutomu Arai, *Japan. J. Appl. Phys.*, **6**, No. 8: 1019 (1967).
15. P.H. Sidles and G.C. Danielson, *Japan. J. Appl. Phys.*, **25**: 58 (1954).
16. S. Nasu, S. Fukushima, T. Ohmichi, and T. Kikuchi, *Japan. J. Appl. Phys.,* **7**, No. 6: 682 (1968).
17. D. Alain, G. Annie, L. Michel, M. Jean-Luc, and S. Gilbert, *C.r. Acad. Sci.*, **B278**, No. 3: 49 (1974).
18. Kubičár L'udovit, *Fys. Čas.*, **22**, No. 3: 129 (1972).
19. M.M. Mebed, R.P. Yurchak, and L.P. Filippov, *High Temp. High Press.*, **5**, No. 3: 253 (1973).
20. D. Murfin, *Rev. Int. Hautes Temp. et Refract.,* **7**, No. 3: 284 (1970).
21. Jean-Claude Weilba-Cher and Jean-Claude van Craeynest, *Rev. Int. Hautes Temp. et Refract.*, **7**, No. 3: 268 (1970).
22. F. Cernuschi, A. Russo, L. Lorenzoni, and A. Figari, *Rev. Sci. Instrum.*, **72**, No. 10: 3988 (2001).
23. G. Wrybel, Z. Rdzawski, G. Muzia, and S. Pawlak, *JAMME,* **36**, 49 (2009).
24. A.V. Lunev and S.A. Pokrovskiy, *Metod Lazernoy Vspyshki dlya Opredeleniya Temperaturoprovodnosti* [Laser Flash Method for Determining Thermal Diffusivity] (Moskva: MIFI: 2003), p. 347 (in Russian).
25. A.D. Falileyev, *Prakticheskaya Realizatsiya Metoda Parkera dlya Opredeleniya Temperaturoprovodnosti* [Practical Implementation of the Parker Method for Determining Thermal Diffusivity] (Tomsk: Izd-vo Tomskogo Politekhnicheskogo Universiteta: 2012), Vol. **3**, Ch. 137, p. 447 (in Russian).
26. V.G. Baranov, A.V. Tenishev, A.V. Lunov, S.A. Pokrovskiy, and A.V. Khlunov, *Yadernaya Fizika i Inzhiniring*, **2**, No. 4: 291 (2011) (in Russian).
27. A.E. Pogorelov, *Metallofiz. Noveishie Tekhnol.*, **36**, No. 3: 383 (2014); https://mfint.imp.kiev.ua/en/abstract/v36/i03/0383.html
28. S.M. Luhuev, N.V. Luhueva, and A.A. Dunaev, *Fiz. Tverd. Tela*, **45**, No. 3: 424 (2003) (in Russian).
29. V.L. Bybyk, *Fundamental'nye Issledovaniya,* No. 6: 49 (2006) (in Russian).
30. V.S. Oskotskiy and I.A. Smirnov, *Defekty v Kristallakh i Teploprovodnost'* [Defects in Crystals and Thermal Conductivity] (Leningrad: Nauka: 1972), p. 160 (in Russian).
31. A.V. Yoffe and A.F. Yoffe, *Fiz. Tverd. Tela*, **2**, No. 5: 781 (1960) (in Russian).
32. G.F. Pogorelova, B.M. Fal'chenko, and A.Ye. Pogorelov, *Metod Opredeleniya Koeffitsienta Diffuzii* [The Method of Determining the Diffusion Coefficient]: Patent 1117491 SSSR (Published 1984) (in Russian).
33. S.D. Gertsriken and I.Ya. Dekhtyar, *Diffuziya v Metallakh i Splavakh v Tverdoy Faze* [Diffusion in Metals and Alloys in the Solid Phase] (Moskva: Fizmatgiz: 1960), p. 563 (in Russian).
34. *Svoistva Elementov: Spravochnik* [Properties of Elements: Handbook)] (Ed. G.V. Samsonov) (Moskva: Metallurgiya: 1976), p. 600 (in Russian).
35. *Svoistva Elementov: Spravochnik* [Properties of Elements: Handbook)] (Ed. M.E. Dryts) (Moskva: Metallurgiya: 1985), p. 672 (in Russian).
36. S.M. Luguev, N.V. Lugueva, and V.V. Sokolov, *Fiz. Tverd. Tela*, **42**, No. 6: 1013 (2000) (in Russian).
37. N.V. Lugueva, N.L. Kramynina, and S.M. Luguev, *Fiz. Tverd. Tela*, **43**, No. 2: 222 (2001) (in Russian).
38. N.V. Lugueva and S.M. Luguev, *Fiz. Tverd. Tela*, **44**, No. 2: 251 (2002) (in Russian).
39. A. Filatov, A. Pogorelov, D. Kropachev, and O. Dmitrichenko, *Defect Diffus. Forum*, **363**: 173 (2015); https://doi.org/10.4028/www.scientific.net/ddf.363.173

40. O.Ye. Pogorelov, A.F. Zhuravlev, and Ye.O. Pogorielov, *Sposib Ekspres-Analizu Teplofizychnykh Kharakterystyk Plivok* [Method of Express Analysis of Thermophysical Characteristics of Films]: Ukrainian Patent 43224A (2002) (in Ukrainian).
41. A. Pogorelov, A. Zhuravlev, Ye. Pogoryelov, and V. Brik, *Metallofiz. Noveishie Tekhnol.*, **23**: 194 (2001).
42. M.E. Gurevich, A.F. Zhuravlev, Yu.V. Kornyushin, and A.E. Pogorelov, *Metallofizika*, **7**, No. 2: 113 (1985) (in Russian).
43. A.T. Kanaev, E.V. Chumakov, and M.T. Toktarkhanov, *Vestnik Kazakhskogo Natsionalnjgo Tekhnicheskogo Universiteta imeni K.Y. Satpaeva*, No. 5 (2008).
44. O.Ye. Pogorelov and K.M. Khranovska, *Sposib Vyznachennia Teplofizychnykh Kharakterystyk Metalevoi Plivky* [The Method of Determining the Thermophysical Characteristics of a Metal Film]: Ukrainian Patent 111801 (2016) (in Ukrainian).
45. U. Paek and A. Kestenbaum, *J. Appl. Phys.*, **44**: 2260 (1973); https://doi.org/10.1063/1.1662547
46. M. Naoe, N. Kitamura, and T. Hirata, *J. Appl. Phys.*, **61**: 3337 (1987); https://doi.org/10.1063/1.338790
47. A.E. Pogorelov, Ye.A. Pogoryelov, and A.F. Zhuravlev, *J. Magn. Magn. Mater.*, **249**, No. 3: 428 (2002); https://doi.org/10.1016/S0304-8853(02)00463-8
48. H. Gonska, W. Kiershpe, and R. Kohlhaas, *Z. Naturforsh.*, **B23a**: 783 (1968).
49. A.F. Zhuravlev, A.E. Pogoryelov, and K.P. Ryaboshapka, *Metallofiz. Noveishie Tekhnol.*, **24**: 1547 (2002) (in Russian).
50. A.E. Pogoryelov, K.P. Ryaboshapka, and A.F. Zhuravlev, *J. Appl. Phys.*, **92**: 5766 (2002); https://doi.org/10.1063/1.1512972
51. A.E. Pogoryelov, K.P. Ryaboshapka, and A.F. Zhuravlev, *Defect and Diffusion Forum*, **216−217**: 41 (2003); https://doi.org/10.4028/www.scientific.net/DDF.216-217.41
52. J.C. Jaeger, *Notes Australian National University*, **XI**, No. 1: 132 (1953).
53. D.S. Svinukhov, V.S. Zhdanov, V.V. Baklanov, and V.V. Sabluk, *Vestnyk NIaTs RK*, No. 2: 86 (2009) (in Russian).
54. E.M. Rudenko, V.M. Sorokin, I.V. Korotash, D.Yu. Polotsky, A.O. Krakovny, O.Yu. Suvorov, M.A. Belogolovskii, and D.V. Pekur, *Dopov. Nac. Akad. Nauk Ukr.*, No. 3: 59 (2018) (in Ukrainian); https://doi.org/10.15407/dopovidi2018.03.059
55. E. Rudenko, I. Korotash, M. Dyakin, D. Polotsky, M. Belogolovskii, and Yu. Strzhemechny, *Proc. 'XI Int. Scientific and Practical Conference on Electronics and Information Technologies'* (*Sep. 16−18, 2019, Lviv*), p. 253.
56. E. Rudenko, Z. Tsybrii, F. Sizov, I. Korotash, D. Polotskiy, M. Skoryk, M. Vuichyk, and K. Svezhentsova, *J. Appl. Phys.*, **121**, No. 13: 135304 (2017); https://doi.org/10.1063/1.4979858
57. Z. Tsybrii, F. Sizov, M. Vuichyk, I. Korotash, and E. Rudenko, *Infrared Phys. & Technol.*, **107**: 103323 (2020); https://doi.org/10.1016/j.infrared.2020.103323
58. Z. Tsybrii, F. Sizov, M. Vuichyk, K. Svezhentsova, E. Rudenko, I. Korotash, and D. Polotskiy, *Advances in Thin Films, Nanostructured Materials, and Coatings. Lecture Notes in Mechanical Engineering* (Eds. A. Pogrebnjak and V. Novosad) (Singapore: Springer: 2019), p. 235; https://doi.org/10.1007/978-981-13-6133-3_24

59. A. Jacquot, B. Lenoir, A. Dauscher, P. Verardi, F. Craciun, M. Stölzer, M. Gartner, and M. Dinescu, *Appl. Surf. Sci.*, **186**, No. 1: 507 (2002); https://doi.org/10.1016/S0169-4332(01)00767-X

60. Y. Zhao, C. Zhu, S. Wang, J.Z. Tian, D.J. Yang, C.K. Chen, H. Cheng, and P. Hing, *J. Appl. Phys.*, **96**: 4563 (2004); https://doi.org/10.1063/1.1785850

61. P.K. Kuo, G.W. Auner, and Z.L. Wu, *Thin Solid Films*, **253**: 223 (1994).

62. T.S. Pan, Y. Zhang, J. Huang, B. Zeng, D.H. Hong, S.L. Wang, H.Z. Zeng, M. Gao, W. Huang, and Y. Lin, *J. Appl. Phys.*, **112**: 044905 (2012); https://doi.org/10.1063/1.4748048

63. S.-M. Lee and D.G. Cahill, *J. Appl. Phys.*, **81**: 2590 (1997); https://doi.org/10.1063/1.363923

64. D.G. Cahill, K. Goodson, and A. Majumdar, *J. Heat Transf.*, **124**: 223 (2002); https://doi.org/10.1115/1.1454111

65. S.R. Choi, D. Kim, S.-H. Choa, S.-H. Lee, and J.-K. Kim, *Int. J. Thermophys.*, **27**: 896 (2006); https://doi.org/10.1007/s10765-006-0062-1

66. C. Duquenne, M.-P. Besland, P.Y. Tessier, E. Gautron, Y. Scudeller, and D. Averty, *J. Phys. D: Appl. Phys.*, **45**: 015301 (2012); https://doi.org/10.1088/0022-3727/45/1/015301

67. E.M. Rudenko, A.O. Krakovnyy, M.V. Dyakin, I.V. Korotash, D.Yu. Polots'kyy, and M.A. Skoryk, *Metallofiz. Noveishie Tekhnol.*, **44**, No. 8: 989 (2022) (in Ukrainian); https://doi.org/10.15407/mfint.44.08.0989

68. E.M. Rudenko, V.Ye. Panarin, P.O. Kyrychok, M.Ye. Svavilnyi, I.V. Korotash, O.O. Palyukh, D.Yu. Polotskyi, and R.L. Trishchuk, *Prog. Phys. Met.*, **20**, No. 3: 485 (2019); https://doi.org/10.15407/ufm.20.03.485

69. V.F. Semenyuk, V.F. Virko, I.V. Korotash, L.S. Osipov, D.Yu. Polotsky, E.M. Rudenko, V.M. Slobodyan, and K.P. Shamrai, *Probl. At. Sci. Technol.*, No. 4 (86): 179 (2013).

70. L. Osipov, E. Rudenko, V. Semenyuk, I. Korotash V. Odinokov, G. Pavlov, and V. Sologub, *Nanoindustriya*, No. 2: 4 (2010) (in Russian).

71. A. Shpak, E. Rudenko, I. Korotash, V. Semenyuk, V. Odinokov, G. Pavlov, and V. Sologub, *Nanoindustriya*, No. 4: 12 (2009) (in Russian).

72. I. Korotash, V. Odinokov, G. Pavlov, E. Rudenko, D. Polotsky, V. Semenyuk, and V. Sologub, *Nanoindustriya*, No. 4: 14 (2010) (in Russian).

73. V.F. Semenyuk, Eh. M. Rudenko, I.V. Korotash, L.S. Osipov, D.Yu. Polotskiy, K.P. Shamray, V.V. Odinokov, G.Ya. Pavlov, and V.A. Sologub, *Metallofiz. Noveishie Tekhnol.*, **33**, No. 2: 223 (2011) (in Russian).

74. I.P. Zharkov, A.N. Ivashchenko, E.M. Rudenko, I.V. Korotash, A.A. Krakovnyy, V.V. Safonov, and V.A. Khodunov, *Science and Innovation*, **7**, No. 2: 5 (2011).

75. S. Zeng, Z. Liu, J. Jiang, M. Jean, and S. Yang, *Am. Ceram. Soc. Bull.*, **95**, No. 5: 38 (2016).

76. H.S. Carslaw and J.C. Jaeger, *Conduction of Heat in Solids* (New York: Oxford University Press: 1959), p. 101.

77. A.E. Pogoryelov and A.V. Filatov, Resistance of Layered Structures to Efficient Transmission of Thermal Energy, *Proc. Sci. Conf. 'Functional Materials for Innovative Energy' (May 13–15, 2019, Kyiv)*, p. 23.

78. S.Yu. Mesnyankin, A.G. Vikulov, and D.G. Vikulov, *Phys.-Usp.*, **52**, No. 9: 891 (2009); https://doi.org/10.3367/UFNe.0179.200909c.0945

79. R.J. Stoner and H.J. Maris, *Phys. Rev. B*, **48**: 16373 (1993);
https://doi.org/10.1103/PhysRevB.48.16373

80. Masahiro Susa, Kazuhiro Nagata, and Kazuhiro S. Goto, *J. Japan Inst. Metals.*,
53, No. 5: 543 (1989); https://doi.org/10.2320/jinstmet1952.53.5_543

81. Y.L. Zhang, C.L. Hapenciuc, E.E. Castillo, T. Borca-Tasciuc, R.J. Mehta,
C. Karthik, and G. Ramanath, *Appl. Phys. Lett.*, **96**, No. 6: 062107 (2010);
https://doi.org/10.1063/1.3300826

82. B.E. Belkerk, J. Camus, B. Garnier, H. Al Brithen, S. Sahli, and M.-A. Djouadi,
Int. J. Therm. Sci., **151**: 106259 (2020);
https://doi.org/10.1016/j.ijthermalsci.2019.106259

О.Є. Погорелов, О.В. Філатов, Е.М. Руденко, І.В. Короташ, М.В. Дякін
Інститут металофізики ім. Г.В. Курдюмова НАН України,
бульв. Академіка Вернадського, 36, 03142 Київ, Україна

МЕТОДИ ВИЗНАЧЕННЯ ХАРАКТЕРИСТИК
ТЕПЛОВИХ ПОТОКІВ У ТВЕРДИХ ТІЛАХ

Завдяки аналізу широкого спектру відомих методів характеризації теплових властивостей твердого тіла визначено найбільш ефективні стосовно дослідження багатошарових систем. Серед розглянутих стаціонарних, квазистаціонарних і нестаціонарних методів виділено Паркерів експрес-метод визначення теплофізичних характеристик пласких об'єктів, 3ω-метод та модифікації їх для точкових і планарних досліджень, зокрема плівок. Застосування модифікованого Паркерового експрес-методу для дослідження шаруватих структур уможливило виявлення ефекту нереверсивности теплопередачі у системі Cu/AlN/Al. Такий ефект пояснено особливостями процесів передачі тепла на межі метал–діелектрик залежно від їхніх Дебайових температур і з урахуванням електрон-фононної взаємодії.

Ключові слова: теплопровідність, 3ω-метод, Паркерів експрес-метод, міряння температури, ефект нереверсивности теплопередачі.